UiT
THE ARCTIC UNIVERSITY OF NORWAY

Faculty of sciences and technology, department of geology

How is the carbon and oxygen isotope composition of foraminiferal tests influenced by methane seepage?

Kine Liland Bruvik

Master thesis in Geology [Geo-3900] , June 2019

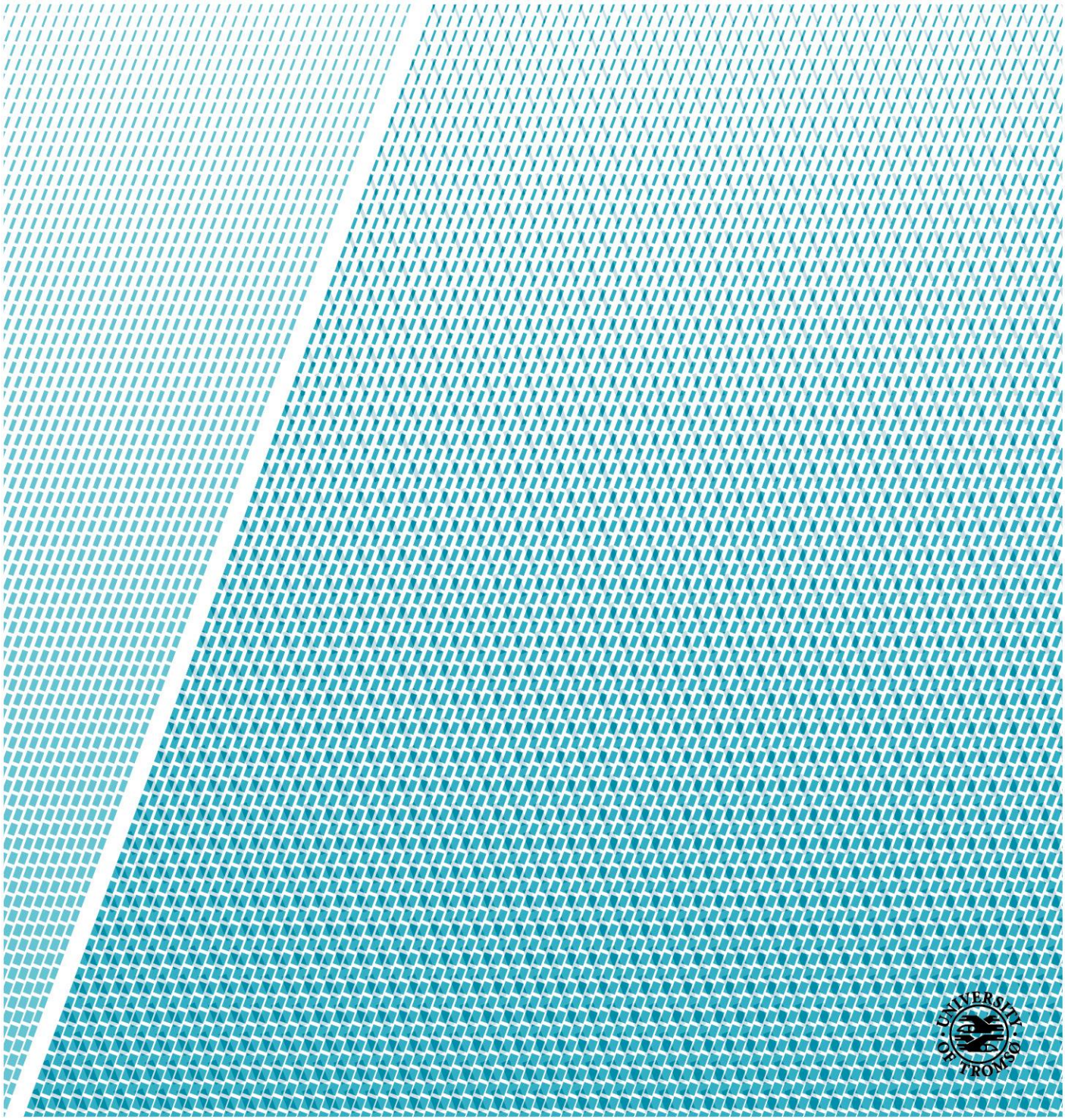

Abstract:

The focus of this thesis is how methane seepage influences foraminiferal tests. Specifically, how carbon and oxygen isotopes in planktic foraminifera tests are influenced by methane seepage. The study area is Vestnesa Ridge were four gravity cores were collected during a CAGE cruise in 2013. The cores were taken both from the southern side, where flares have been recorded, and from the northern side, where there are no active seepage areas.

The cores were worked on in the lab, samples were taken and sieved. After this planktic *(Neogloboquadrina pachyderma s/d*) and benthic *(Cassidulina neoteretis)* foraminifera were picked. Isotope analyses were done on planktic *(Neogloboquadrina pachyderma s/d*) foraminifera, providing the carbon ($\delta^{13}C$) and oxygen ($\delta^{18}O$) isotope measurements. These values were used to identify if methane seepage affected the cores. Two of the four cores (HH-13-197 and HH-13-215) indicated methane seepage. Both the distinctly negative $\delta^{13}C$ and the magnetic susceptibility data indicated methane seepage for these two cores.

The isotope signals were used to identify past SMTZ, while the present SMTZ were found in core HH-13-197 from pore water data showing sulphate measurements.

Acknowledgements:

There are many people who deserves gratitude for all they have done to help with this thesis. My supervisor Giuliana Panieri how has been guiding me from start to the end, with suggestions, pointers, questions and a lot of knowledge. Thank you for all the help both during the laboratory work in Tromsø and during the writing of the thesis.

I want to thank Andrea Schneider how was my co supervisor at the start of the thesis, you checked up on me a lot during the lab work and I could always ask if there was something I did not understand. This was extremely helpful and made sure that the lab work went very smoothly. Thank you for the support and helpful advices along the way.

Thanks to Chiara Borrelli for steeping in as co supervisor at the end. You have been very helpful with all your feedback and advices, which I am very thankful for.

I need to give a thanks to CAGE for the cores and all the work that already had been done on them, the x-rays, pore water measurements (core HH-13-197), and magnetic susceptibility data. It has been of great value to be able to use this data in the thesis.

I want to thank all the employees that work at the lab in Tromsø, Karina Monsen, Trine Dahl, Ingvild Hald and Matteus Lindgren. Thanks for all the help and assistance, I want to thank Matteus Lindgren for the isotopic analysis of the samples.

A big thank to my fellow students that worked in the lab, we had a lot of good discussion. An special thanks to Felix, Anne and Anette for a lot of fun and good conversations during the lab work.

I also want to thank my family for being patient and for babysitting so I could finish my thesis. I want to thanks my love who always is supporting and helpful.

Thank you all very much.

Kine Liland Bruvik

Table of Contents

List of Tables

List of Figures

1 Introduction:

1.1 Objective:

The main objective of this master project is to investigate possible past methane seepage events in pockmarks along Vestnesa Ridge, in the Fram Strait. The study focuses on oxygen and carbon isotope measured in planktic foraminiferal calcareous shells. These data will contribute to improve the knowledge of methane history at Vestnesa Ridge during the Pleistocene.

1.2 Background:

1.2.1 Western Svalbard continental slope:

The Western Svalbard continental slope consists of glacigenic Through-Mouth fans and inter-fan areas, that were formed during the Late Pliocene and Quaternary on top of oceanic basement (Howe et al., 2008; Jessen et al., 2010). In the Through-Mouth fans there are thick mass of transported sediments deposited during full glacial condition, mainly debris flows and turbidites. Thin layers of the mass transported sediments are also found in the inter-fan areas. Above these mass transported deposits there are hemipelagic sediments. Hemipelagic sediments are also found in between the fans, along with sediment drifts. Along the slope at 1000-3000m depth, bottom current activity generated contourites: this process has been going on for at least 3 million years (Jessen et al., 2010). One of these contourites were deposited in the late Quaternary period. It is situated at 1200-1300m water depth and at 79°N: this is the Vestnesa Ridge.

1.2.2 Climate and oceanography:

The northward transport of warm Atlantic surface water is responsible for the mild winter climate in northwestern Europe. This warm surface water is part of the global thermohaline conveyor belt and contributes to the formation of the North Atlantic Deep Water (NADW) (Brix & Gerdes, 2003; Howe et al., 2016; Jessen et al., 2010; Rudels, 2015). In the Fram Strait the upper 500-700m of the water column consists of warm Atlantic water. Deeper than 700m depth the water masses consist of intermediate and deep waters that are generated by convention in the Nordic Sea. The deeper laying water masses have a temperature of -1ºC and are denser than the surface water because they are more saline. The convection occurs due to cooling of the surface water, this cooling is done by cold winds from Greenland and by contact with sea ice. The formation of sea ice also contributes to saltier water masses. This

colder, saltier surface water is denser and therefore starts to sink. The convection recirculates the Atlantic surface water that flow southwards as a deep current below the cold East Greenland current.

The Fram Strait has two main currents, the West Spitsbergen Current (WSC) and the East Greenland Current (EGC). The WSC is a branch of the warm Atlantic surface water that continues along the Western Svalbard margin and in to the Arctic Ocean as The Yermak Slope Current (Howe et al., 2008; Jessen et al., 2010). As the Yermak Slope Current goes into the Arctic Oceans it continues as a subsurface current below the low salinity Polar water mass. The upper 500m of the WSC current is deflected eastwards by the Coriolis force, becoming the North Spitsbergen Current (NSC). It flows towards the north of Svalbard. The Fram Strait is also affected by the East Greenland Current (EGC) which flows along the bottom ocean of the Greenland margin. This current moves polar water southward along the Greenland margin. The Svalbard margin is therefore affected by both the warm Atlantic surface water and the cold low salinity Polar surface water.

1.3 Study area:

1.3.1 Vestnesa Ridge:

Vestnesa Ridge is situated in the Fram Strait 79ºN and between 06ºE and 07ºE, and it is the only deep-water connection between the Arctic Ocean and the North Atlantic Ocean (Bradley, 2015; Brix & Gerdes, 2003; Howe et al., 2008; Jessen et al., 2010; Rudels, 2015). The deepest point here is the Molloy Deep, more than 5000m deep. Because this area is in the middle of the average winter/summer sea ice boundary, the sediments are influenced by both the global thermohaline circulation and ice sheets melting.

The sediment drift which constitutes Vestnesa Ridge is approximately 100km long and bends SE–NW to E–W. Its sediments are over 2km thick and were developed by contour drift along the Western Svalbard margin at water depth of 1200-1300m (Howe et al., 2008). The Western Svalbard margin is a passive margin, characterized by complex and tectonic active movements with transform faults and ultraslow spreading ridge systems (Johnson, 2015; Plaza-Faverola et al., 2015). The upper sediment of Vestnesa Ridge, consists of sediments deposited in the Late Pleistocene and Holocene and are composed of silty contourites, turbidites and hemipelagites with abundant ice rafted debris (Howe et al., 2008; Howe et al., 2016; Vogt et al., 1999). The contourite is of late Quaternary age, it contains sediments deposited mostly during the late Miocene and Pleistocene (Jessen et al., 2010; Schneider et

al., 2018; Vogt et al., 1999; Vogt et al., 1994). The oceanic basement below Vestnesa Ridge is <20 Ma old and consists of oceanic crust (Hustoft et al., 2009).
The crest of the Vestnesa Ridge is characterized by gas related structures and active and inactive pockmarks. The active pockmarks form where there is highly localized fluid seepage occurring in unconsolidated fine-grained sediments (Vogt et al., 1994; Judd & Hovland, 2007). Pockmarks on Vestnesa Ridge have different size, and can reach up to 700m in diameter (Bünz et al., 2012). Currently, the methane that is escaping from the pockmarks originated from the decay of organic matter deposited during Miocene age. Gas hydrates has also been found along the Ridge within some of the active pockmarks (Panieri et al., 2016; Schenider et al., 2018). Seismic studies indicate that multiple seepage episodes have occurred during the past 2.7Ma being closely linked to fault reactivation and fracturing (Plaza-Faverola et al., 2015).

1.4 Methane:

Methane (CH_4) is probably the most abundant and widespread hydrocarbon gas found within marine sediments. It is the lightest and simplest of the hydrocarbon gases (Hovland & Judd, 1988; Whiticar, 1999). Methane can be released also from gas hydrates, as a result of instability, when the temperature and pressure conditions which are required to form and keep hydrates stable are lost. This process is named “dissociation”.

Methane is produced mainly through microbial processes (methanogenesis). The methane concentration in sediments is measured as a function of the sediment depth. The concentration is usually low at the surface and increase with depth. In the methanogenic zone there is bubble formation when the methane concentration is near the pore-water saturation level (Hovland & Judd, 1988; Whiticar, 1999). The methane produced in this zone has a low $\delta^{13}C$ values (-70‰ to -90‰) and a relatively high concentration. At the bottom boundary of the methanogenic zone the concentration is between 60% and 100% (figure 1).

It is very important to understand where the methane is oxidized (consumed) because this process regulate the quantity of methane that reaches the seafloor and potentially the atmosphere. The methane oxidation occurs both aerobically and anaerobically. In the next chapter I am going to explain how these processes occur.

1.4.1 Aerobic oxidation:

During the process of aerobic oxidation, there is a group of enzymes that use methane as a source of energy and carbon and oxidized it using oxygen molecules (Zehnder & Brock, 1979). These aerobic organisms are assumed to have a main role in the oxidation of methane in the upper layers of sediments (Sundh et al., 1995). The aerobic methanotrophic organisms are dependent on oxygen and methane, therefore the abundance and activity of these organisms usually is highest near the interface between anoxic and oxic conditions. The main oxidation product from the oxidation of methane is CO_2 (Zehnder & Brock, 1979).

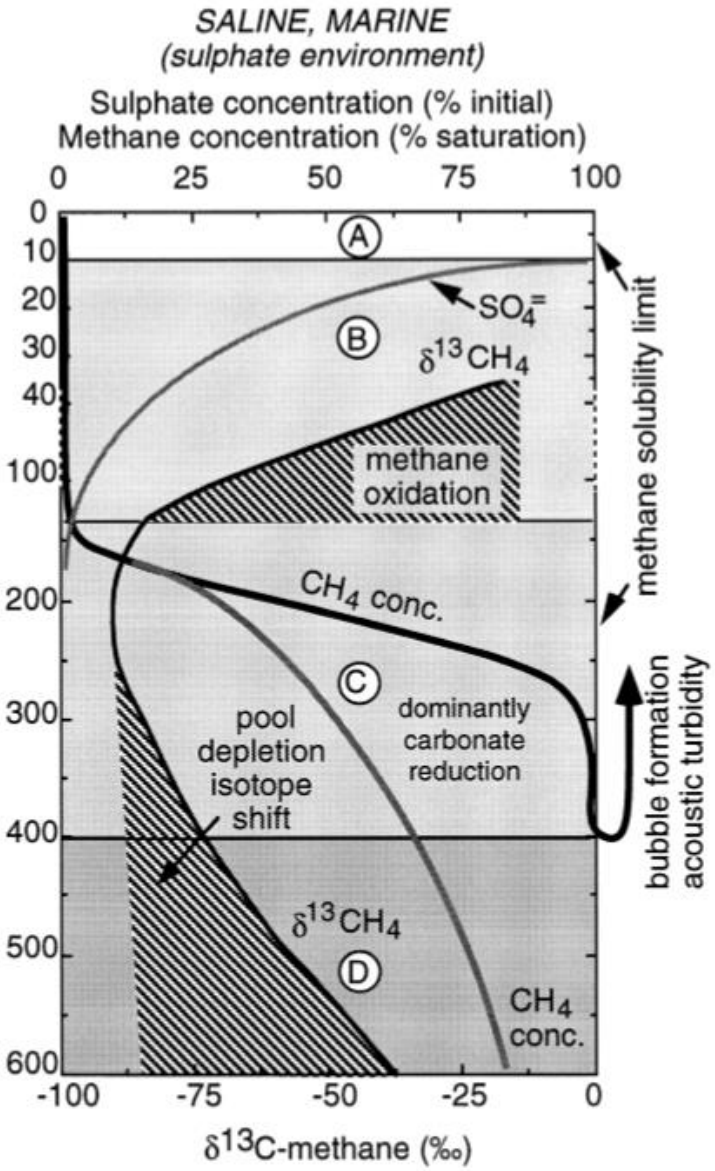

Figure 1 From Whiticar (1999)– Sediment depth profile of methane concentration, sulphate concentration, and carbon isotope composition. A = oxic zone, B = sulphate reduction zone, C = methanogenic zone, and D = substrate depletion and / or carbonate reduction zone.

1.4.2 Anaerobic oxidation:

Anaerobic Oxidation of Methane (AOM) has been identified in marine environments, mainly coupled to sulphate reduction. The sulphate reduction zone, which is found above the methanogenic zone in the sediments (figure 1), is where the methane concentration is very low, while the sulphate concentration starts very high (100%) in the shallower parts and gets lower with depth (<1%) (figure 1) (Whiticar, 1999). This one is also named sulphate methane transition zone (SMTZ) and it is where much of the methane that is produced in marine sediments is converted into CO_2 by anaerobic oxidation, results of archaea that reverses the methanogenesis by interacting with sulphate-reducing bacteria. One of these sulphate-reducing bacteria is *Beggiatoa* , which very often is found in combination with *clams* that at the seafloor indicates areas of active gas seeping. One study by Boetius et al. (2000) at Cascadia convergent margin (located off the coast of Oregon) studied sites which were covered in *Beggiatoa mats* and found that the areas had an extremely high sulphate reduction rate (SRR), reaching more than 5 mmol cm^{-3} d^{-1} in the surface sediments. This very high SRR value were measured at Hydrate Ridge (44°34′ N, 125°09′ W, 780m water depth), were the sulphate reduction was influenced by high methane fluxes rising from deeper parts of the sediments. A reference point with no vents or hydrates near the Ridge shows this influence as the SRR was below the detection limit (<1 nmol cm^{-3} d^{-1}) (Boetius et al., 2000). There was no methane here to fuel the sulphate reduction. These very high SRR values have been found to be restricted to sediments rich in methane. It has been proposed that sulphate is the terminal electron acceptor in the AOM zone.

$$CH^4 + SO_4^{2-} \rightarrow HCO_3^- + HS^- + H_2O$$

The equation above shows sulphide as a product of the anaerobic oxidation of methane, it can accumulate to almost the equivalent of what the sulphate can consume. This sulphide production can explain the occurrence of the *Beggiatoa* communities at Hydrate Ridge, as they are sulphide based. Both the archaea and the *Beggiatoa* covered sediments on the Hydrate Ridge were found being highly depleted in ^{13}C (-124‰ and -114‰ to -133‰) (Boetius et al., 2000). These highly depleted ^{13}C values are due to consumption of methane. Sulphate reduction is a normal process that occurs in the sediments and causes degradation of organic matter.

1.4.3 C and H isotope variations of methane:

Isotopic measurements of methane from both ancient and recent sedimentary records give the possibility to distinguish between microbial and thermogenic methane types. This is done by using carbon and hydrogen stable isotopes: $\delta^{13}C_{CH4}$ and δD_{CH4} respectively. The C and H isotope data was used to make a CD diagram with classification of microbial and thermogenic methane.

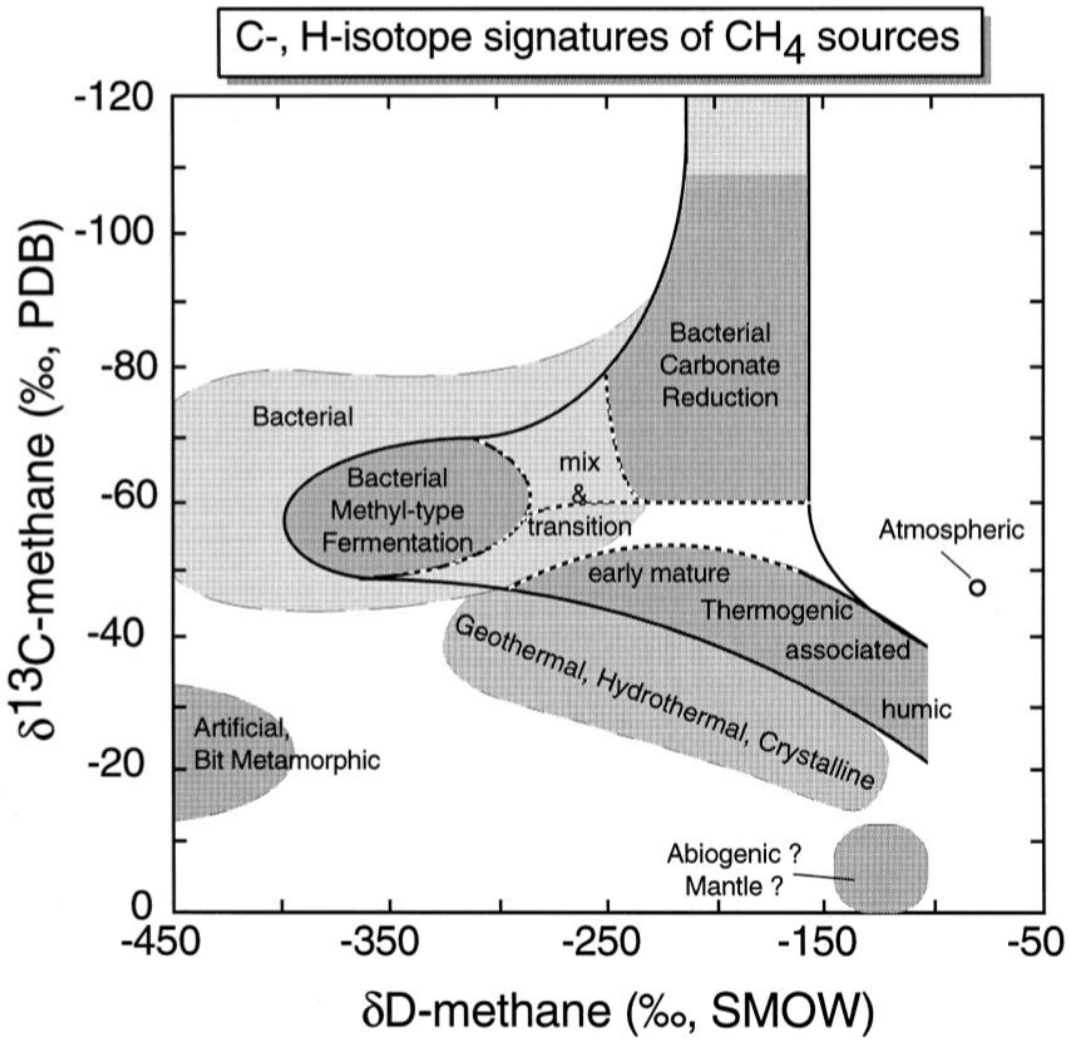

Figure 2 From Whiticar (1999) – a CD-diagram for classification of microbial and thermogenic methane from the combination of $\delta^{13}C_{CH4}$ and δD_{CH4} information.

1.4.4 Microbial methane:

Microbial methane is produced from an end product of decomposed organic matter, which involves diverse microorganisms. The end product is methanogenic archaea (Judd et al., 2002). Shortly after the deposition of organic matter the process will occur. This process usually occur at relatively shallow depths within the sediments, where sulphate reducing bacteria have depleted the sulphate level (Malinverno, 2010). Microbial CH_4 has carbon

isotope values ($\delta^{13}C_{CH4}$) between -50‰ to -110‰, while the hydrogen isotope values (δD_{CH4}) vary between -150‰ to -400‰ (figure 2) (Whiticar, 1999). Carbon reduction is the main methanogenic pathway in marine environment while acetate fermentation is more important in freshwater environments.

1.4.5 Thermogenic methane:

Thermogenic methane is often enriched in ^{13}C when compared with microbial methane. It has a $\delta^{13}C_{CH4}$ values of about -50‰ to -20‰ (Whiticar, 1999). Usually the thermogenic generation of hydrocarbons occurs at a higher temperature compared to the microbially-generated methane. The different thermogenic gases can be classified according to the source rock (kerogen type) maturity level. As the maturity level increases, the thermogenic gases will become more enriched in $\delta^{13}C_{CH4}$. It will eventually approach the $^{13}C/^{12}C$ of the original organic matter or kerogen. The carbon isotope variation between thermogenic and microbial methane is between 0-30‰. While the hydrogen isotope rations δD_{CH4} can be between -100‰ to -275‰ for thermogenic methane (Whiticar, 1999). The δD_{CH4} values for microbial methane range from -150‰ to -400‰ and for thermogenic methane do the δD_{CH4} range from -100‰ to -275‰ (figure 2). These values has some overlap and it will therefore be useful to use molecular or isotope composition data in addition to the δD_{CH4} values.

1.5 Processes occurring at the SMTZ:

In the marine sediment where methane rises from free gas or from gas hydrate dissociation, there is a very peculiar feature in the geochemical environment: it is the presence of methane-derived ^{13}C-depleted dissolved inorganic carbon (DIC). In sediments exposed to methane seepage, a microbial consortium consisting of archaea and sulphate-reducing bacteria mediates anaerobic oxidation of methane (AOM) (Boetius et al., 2000). Methane-derived DIC is produced by the AOM and its geochemical signature is preserved in authigenic carbonates which precipitates due to local supersaturation of carbon at SMTZ (Panieri et al., 2016; Whiticar, 1999). AOM occurs close to seawater-sediment interface during high methane fluxes. The methane flux is what controls the depth of the SMTZ. At the SMTZ several chemical reactions occur, and are related to the microbial activities:

$$1: CH_4 + SO_4^{2-} \rightarrow HS^- + HCO_3^- + H_2O$$

$$2: 2HCO_3^- + Ca^{2+} \rightarrow CaCO_3 + CO_2 + H_2O$$

$$3: CH_4 + 2O_2 \rightarrow CO_2 + 2H_2O$$

The first equation shows the AOM that occurs when methane rises into the SMTZ and encounters sulphate. In the near-seafloor sediments, up to 90% of the methane can be consumed by anaerobic oxidation of methane (AOM) by a consortium of methanotrophic archaea and sulphate-reducing bacteria. The second equation shows the production of bicarbonate from AOM; this bicarbonate can induce the precipitation of authigenic carbonates due to local supersaturation of carbonate. These methane-derived authigenic carbonates can precipitate in different shapes like crusts, nodules, and chimney. They show typical negative $\delta^{13}C$ values (Greinert et al., 2001). AOM that occurs close to the seawater-sediment interfaces caused by high methane fluxes, establishes benthic communities that includes bacterial mats that do sulphide oxidation and benthic aerobic oxidation of methane in the deep waters at the ocean bottom. This benthic aerobic oxidation of methane is showed in the third equation.
At the SMTZ, the hydrogen sulphide produced by AOM promotes dissolution of detrital magnetite. This leads to a reduction in the solid phase of the sediments oxides which can cause a decline in magnetic susceptibility profiles. This change in magnetic susceptibility depends on how much detrital magnetite is left and for how long the SMTZ resides at a given sediment interval, on the sedimentation rates and methane flux.

1.6 Gas hydrates:

Gas hydrates are ice-like structures formed by a mixture of gas and water molecules. The hydrogen bonded water molecules contain the gas molecules in a cage-like structure. This structure is formed within sediments that contain both water and gas under low temperature and high pressure conditions (Judd et al., 2002; Ruppel & Kessler, 2017; Smith et al., 2014). Gas hydrates are therefore formed in environments, where the surface temperature is below 0°C and at the sea bottom in the seabed where the temperature is less than 5°C and the water depth exceeds 300m at high latitudes and 500m at temperate latitudes (Judd et al., 2002; Ruppel & Kessler, 2017). These depth marks the shallowest Pressure-Temperature (PT) limit where the GHSZ can exist on the slope of continental margin. These conditions are often found in polar regions. Most hydrates formed on continental margins where there are large enough concentrations of methane produced by the decomposition of organic carbon, transported to the sediments by sink of phytoplankton and by export of terrestrial sediments from the continents.

Gas hydrates usually contain methane gas. The sources of this methane may be from shallow microbial sources, and they have a methane content of >99% (Klitzke et al., 2016). It can also form with thermogenic gas that flowed up from deeper leaked petroleum systems, this gas

contains between 25-99% of methane. Another potential source is abiotic methane that comes from mantle serpentinization of ultramafic rocks. Gas hydrates may represent the greatest reservoir of methane (Judd et al., 2002).The estimates vary, but there has been suggested that the global amount of methane hydrate may be towards the lower to intermediate parts of the range 10^{15} to $10^{17}m^3$. Methane from gas hydrates can be released if there are changes in temperature or pressure conditions and the hydrate loses its stability.

It has been suggested that the gradually warming of oceans can lead to dissociation of hydrates stored along the continental margins. An example is in the Arctic and offshore the Eastern U.S. where this may result in massive escape of methane from gas hydrate dissociation that it is released into the oceans (Smith et al., 2014). In the past, hydrate dissociation and consequent methane release could have caused slope failures.

Hydrate stability zone:

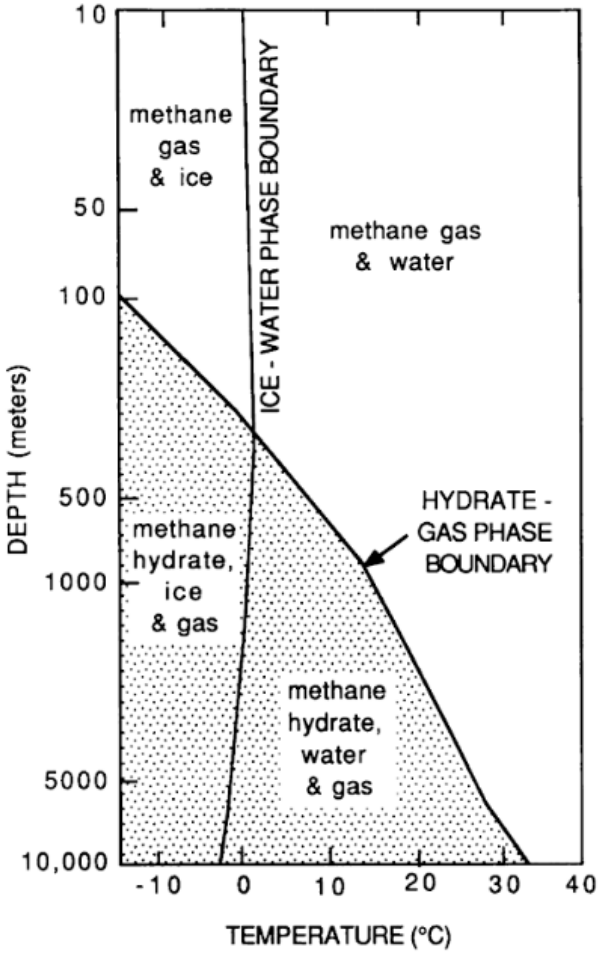

Figure 3 From Vorren et al (1990) – Shows the hydrate pressure-temperature stability field. As basal ocean water is generally below 2.5 degrees Celsius will all ocean depths that are below 400m be a stable zone for hydrate formation.

The Gas Hydrate Stability zone (GHSZ) is the zone in the sediments where the gas hydrates are stable (figure 3) (Ruppel & Kessler, 2017; Vorren et al., 1990). It is the zone where the temperature and pressure conditions make it possible for hydrates to form. When the lower part of the GHSZ moves upward because of continuing sedimentation, free gas starts to raise because gas hydrates become unstable. The sedimentation forces the lower part of GHSZ to move upward to keep the thermodynamic system in balance (Vorren et al., 1990). Heat from deeper within the sediments raises the temperature in the sediments beneath the new GHSZ, making the gas hydrates unstable so that they dissociate releasing gas (Vorren et al., 1990). It is a process where gas concentrates in the GHSZ or in gas pools below. Therefore gas that is produced in ocean sediments will tend to migrate upward into the uppermost part of the sediment column. Thus, the only way that gas can escape the hydrate cap and possibly reach the water column is if it gets through the hydrate layer.

The hydrate layer is at a steady state, thus the gas produced in this layer or below it will become trapped in the GHSZ in the uppermost sediments. Usually the upper boundary of the GHSZ is close to or at the ocean bottom, below 200-400m water depth (Vorren et al., 1990). Hydrates with up to 1100m thickness were observed on the continental shelf and deep ocean. The thickness of the GHSZ at constant geothermal gradients increases as the water depth and pressure increases.

Pockmarks are easily recognisable on the ocean floor and often indicates gas and gas escape. They are therefore often used to indicate concentrations of gas in the GHSZ, that are held in metastable reservoirs. Even though the hydrate can keep the gas concentrated at a depth below the ocean floor, the gas will be able to break through at some locations.

1.6.1 Pockmarks and flares:

Pockmarks are craters formed on the seabed in soft sediments by gas and were first described by King and MacLean in 1970 shortly after the invention of side-scan sonar. The pockmarks where discovered on the continental shelf off Nova Scotia, Canada. Shortly after, pockmarks were also discovered in the North Sea (Hovland & Judd, 1988). King and MacLean proposed the hypothesis that pockmarks were a result of fluid or gas escape, which is still valid today. As pockmarks leaves characteristic marks in marine mud on the seabed, they can be used to indicate seepage sites. Seabed seepage sites are found widely spread both on the continental shelf, continental slope and offshore. They may release hydrocarbon, hydrothermal or volcanic fluid/gas, or groundwater. The bathymetry of Vestnesa Ridge shows a lot of

pockmarks along the ridge. Many of them are hundreds of meters in diameters (ca 500) and up to 20-30m deep (Smith et al., 2014). In 2008 there was the first report of gas bubbles (flares) coming from some of the pockmarks (Schiermeier, 2008). Flares can be detected by using an echosounder, that sends acoustic signals on the ocean bottom where they are then reflected.

2 Foraminifera

Foraminifera are a group of calcareous marine organism. Specifically, they are single-cell protozoa that can live in the water column (planktic foraminifera) or at the sediment/water interface, inside the sediment, or attached to a substrate (benthic foraminifera) (Bradley, 2015). Foraminiferal cells are surrounded by a test. The test can consist of one or multiple chambers and it can have one (foramen) or several (foramina) openings. (Armstrong & Braiser, 2013) The foraminiferal cell is divided into an outer layer of ectoplasm and an inner layer of endoplasm. The ectoplasm forms pseudopodia, which is a temporary or semipermanent extension of the cytoplasm. They are used during feeding or locomotion, when feeding are the pseudopodia used to either trap prey or engulf it. The endoplasm contains either a single nucleus or multiple nucleus, food vacuoles, and small organelles. In the nucleus are the chromosomes that controls the protein synthesis.

2.1 The test

One of the functions of the foraminiferal test is protection, as it shields the organism from biological, chemical, and physical stress. Some forms of biological stress are worms, crustaceans, gastropods, echinoderms, and fish that may accidently ingest the foraminifera when they feed on detritus at the ocean bottom. The foraminifera may be exposed to chemical stress, like fluctuations in salinity, pH, CO_2, O_2, and some toxins. Physical stress includes the harmful radiations from the sun, water turbulence, and abrasion. The outer chambers may act as protective spaces, so that cytoplasm can retreat into the inner chambers during distress. The tests are also helpful when it comes to buoyancy because tests give negative buoyancy, which is especially helpful for benthic foraminifera. For planktic foraminifera, test surface sculptures, like spines and keels, provide positive buoyancy. Surface sculpture may also

improve adherence, strengthen the test, and facilitate the ectoplasm flow to and from apertures, pores, and umbilicus.

The foraminiferal test can organic, agglutinated, or calcareous. The organic test can be proteinaceous or made of pseudochitinous matter. Agglutinated tests are made of organic and mineral matter connected by an organic, calcareous, or ferric oxide cement. The calcareous test is composed by calcium carbonate precipitated by the foraminifera (Armstrong & Braiser, 2013). Calcareous tests are widely used in paleoceanography and paleoclimatology and are going to be the focus of this thesis.

2.1.1 Calcareous test

Calcareous tests can be porcelaneous imperforate, microgranular, or hyaline perforate (Armstrong & Braiser, 2013). Porcelaneous imperforate tests lack mural pores and appear milky or amber when observed in reflecting or transmitted light, respectively. Thin sections of microgranular tests appear opaque with usually a brown or grey colour when observed with a reflected light. These tests look much darker when observed with a transmitted light. Hyaline perforate tests appear glassy under a reflected light and grey to clear when observed with a transmitted light. The clarity of hyaline perforate tests may be obscured by spines, granules, perforation, pigments and diagenesis (Armstrong & Braiser, 2013).

Calcareous foraminiferal tests are easily preserved in marine sediments and they can be studied to understand the paleoenvironment at the time in which the foraminiferal calcify. For example, planktic foraminifera can be used to reconstruct sea surface temperatures and ocean circulation. Instead, benthic foraminifera can be utilized to study bottom water masses (Consolaro et al., 2018). However, during data interpretation it is important to consider the potential influence of dissolution and diagenesis of the foraminiferal tests (Zamelczyk et al., 2013; Panieri et al., 2017).

2.2 Planktic foraminifera

Planktic foraminifera are the focus of this thesis. Today, there are roughly 100 species of living planktic foraminifera. Planktic foraminifera are usually <100µm, live for about 1 month, and have a test adapted for positive buoyancy (Armstrong & Braiser, 2013). Among the modern species , many reproduce in surface water, whereas they start to slowly sink when reaching the end of adult life. Each species prefers a specific temperature and density range. In the upper 50m of the water column there are shallow species (e.g. *Globigerinoides ruber*) (Schiebel & Hemleben, 2005). These species have long spines and globular chambers with

high porosity (for buoyancy) and secondary chambers (to facilitate symbiont movements). Intermediate species live between 50-100m depth. Among these species, there are spinose forms harbouring symbionts and living in oligotrophic waters (e.g. *Orbulina universa*), and non-spinose forms. These do not have symbionts and live in more eutrophic conditions (e.g. *Globigerina bulloides*). Deeper species live below 100m depth, in cold, dense, and eutrophic waters. Generally, these species are characterized by low test porosity, club-shaped chambers (e.g. *Hastigerinella adamsi*), or the absence of spines. The presence of keels helps delaying sinking (e.g. *Globorotalia menardii*). Because of the low pH and higher pressures typical of deep waters, deeper species have to deal with $CaCO_3$ dissolution, which might explain the extra amount of calcite which is seen in some species (Armstrong & Braiser, 2013).

2.2.1 Temperature and latitude

The modern assemblages of planktic foraminifera can be arranged into different provinces - Arctic, Subarctic, Transitional, Tropical, Subtropical, Transitional, Subantarctic and Antarctic. Most species have a bipolar distribution– i.e., they can be found in their favourite provinces at northern and southern latitudes. Diversity increases towards the tropical province. At higher latitude, in waters with temperatures below 5ºC no keeled forms are found (Armstrong & Braiser, 2013). Near the equator, the test porosity of shallow and intermediate species increases. This may be related to the lower density of warmer water. There is a strong correlation between the planktic foraminiferal distribution and the surface ocean circulation pattern. Thus, it is possible to determine the history of surface ocean circulation and temperature during the Quaternary by studying the distribution of fossil planktic foraminifera.

2.2.1.1 Planktic foraminifera species in the Arctic Ocean and Nordic Seas:

In surface waters of the Arctic Ocean and Nordic Seas there are some characteristic planktic foraminifera species. During colder stadial periods and Heinrich events, the most abundant species is the polar species *Neogloboquadrina pachyderma s*. During warmer periods, interstadials, which are influenced by a higher inflow of warmer North Atlantic surface waters, subpolar planktic foraminifera species are more common. Some of the species found during the warmer periods are *Turborotalita quinqueloba,* which is mainly found in productive Arctic waters or near Arctic/Polar Fronts, *Neogloboquadrina pachyderma d.*, which is found when warm Atlantic Surface waters are present, *Globigerinita uvula,* which is found near Arctic/Polar fronts, upwellings areas and in cold productive surface waters, and *Globigerinita glutinata* and *Globigerina bulloides,* which are both found in warm Atlantic

Surface waters (Consolaro at el., 2018). The modern assemblages of planktic foraminifera in the Nordic Seas consists of *Neogloboquadrina pachyderma s, Turborotalita quinqueloba, Globigerina bulloides, Globigerinita glutinata* (Nieuwenhove at el., 2008).

2.2.2 Neogloboquadrina pachyderma:

Neogloboquadrina pachyderma can either be sinistral (left-handed coiled; polar species) or dextral (right-handed coiled; subpolar species). It has a trochospirally coiled non-spinose test with coarsely perforate chambers and an umbilical aperture. The test has calcite walls and no keel or tooth. It usually occurs in transitional to polar water masses. It thrives in low sea surface salinity with little seasonal changes and colder temperatures. It can also tolerate a wide temperature ratio (Ehrenberg, 1996). Its preference for high latitudes is reflected by its preference for low vertical temperature gradients.

The most abundant planktic foraminifera species found in the Fram Strait and Nordic Seas is the polar species *Neogloboquadrina pachyderma s*. This species is typical for colder Arctic surface waters and Polar surface waters. In the Fram Strait, it more abundant during colder stadial periods and Heinrich events (Rasmussen & Thomsen, 2008). During sea ice free conditions, *Neogloboquadrina pachyderma s.* is usually more abundant below 100m water depth, while during periods with sea ice cover this species is usually found closer to the surface (Carstens at el., 1997).

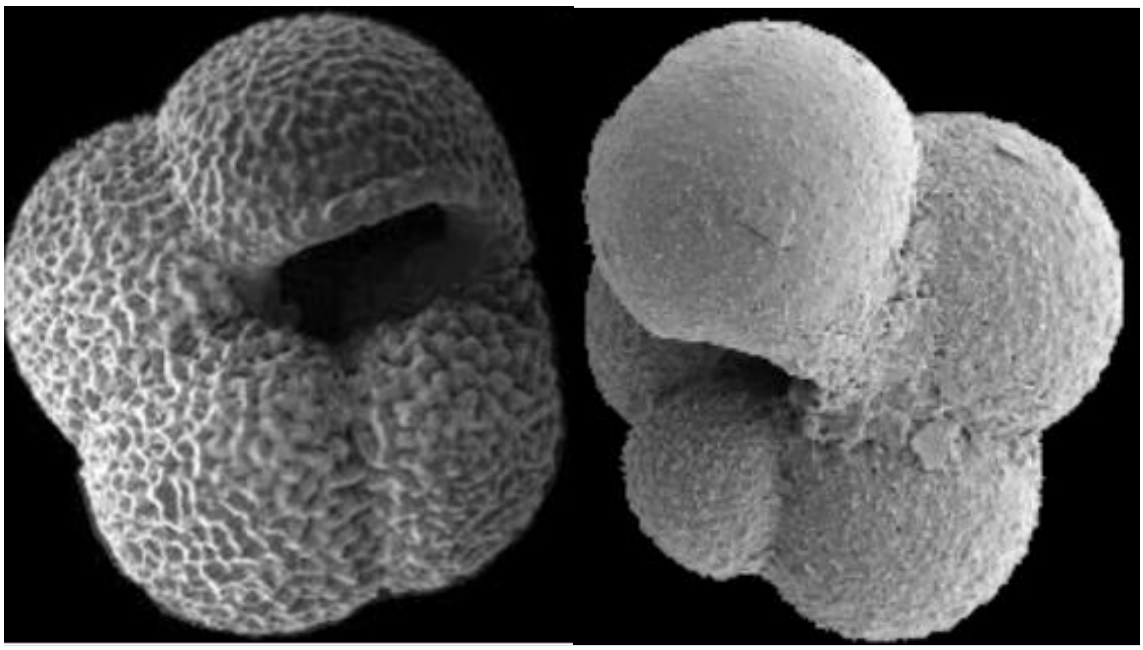

Figure 4 From Ehrenberg (1996) – *Neogloboquadrina pachyderma* sinistral colied (s; on the left) and dextral coiled (d; on the right).

2.2.3 Stable isotopes:

During calcification, elements and isotopes from the surrounding water are incorporated into the foraminiferal test. In particular, the carbon and oxygen isotopes are widely used in palaeoceanography and they can be easily quantified through mass spectrometry. During analysis, data on carbon and oxygen isotopes are obtained at the same time from the same sample. The foraminiferal isotopic composition is reported in delta notation (δ), which represents the ratio between the heavier and lighter isotope of the sample minus the ratio between the heavier and lighter isotopes of the standard, all divided by the ratio between heavier and lighter isotope of the standard, multiplied by 1000:

$$\delta^{13}C = \left(\frac{\left({}^{13}C/{}_{12}C\right)_{sample} - \left({}^{13}C/{}_{12}C\right)_{standard}}{\left({}^{13}C/{}_{12}C\right)_{standard}}\right) \times 10^3$$

$$\delta^{18}O = \left(\frac{\left({}^{18}0/{}_{16}0\right)_{sample} - \left({}^{18}0/{}_{16}0\right)_{standard}}{\left({}^{18}0/{}_{16}0\right)_{standard}}\right) \times 10^3$$

Thus, the δ is expressed in part per thousand (‰). For carbonates, the standard used for analysis of carbon and oxygen isotopes is the Vienna Pee Dee Belemnite (VPDB) (Pearson, 2012).

Considering the focus of this thesis, the sections below describe the processes influencing the isotopic composition of planktic foraminifera.

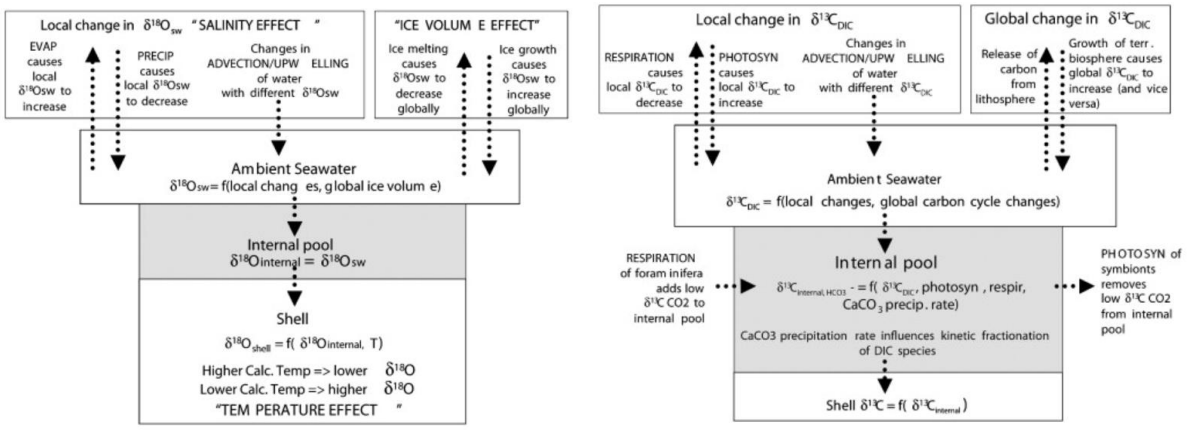

figure 5 From Ravelo & Hillaire-Marcel (2007) – shows the factors that influence the $\delta^{18}O$ (left picture) and $\delta^{13}C$ (right picture) of foraminiferal tests.

2.2.4 Carbon isotopes:

Carbon has two stable isotopes, ^{12}C and ^{13}C, and one non-stable isotope, ^{14}C. ^{12}C is the most abundant carbon isotope (98.9% of the stable carbon on Earth), whereas ^{13}C represents only a minor part (1.1% of the stable carbon on Earth) (Armstrong & Braiser, 2013).

In calcareous foraminifera, the $\delta^{13}C$ of the test depends on the seawater dissolved inorganic carbon (DIC) $\delta^{13}C$ at the time of calcification. However, foraminifera do not calcify in isotopic equilibrium with seawater mostly because of the fast rate of biogenic calcium carbonate precipitation, which leads to kinetic isotope fractionation, and "vital" effects (Ravelo & Hillaire-Marcel, 2007). $\delta^{13}C$ of the tests can be used to reconstruct methane seepage because of AOM which promotes precipitation of methane-derived authigenic carbonate (MDAC), and influences the $\delta^{13}C$ values so that they get distinctly negative. These distinctly negative values indicate past SMTZ, were AOM occurs. Since MDAC provides evidence of AOM, the foraminifera tests affected by this are indicative of methane seepage.

The $\delta^{13}C$ of seawater DIC is not constant. On a shorter time scales, different oceans are characterized by different DIC $\delta^{13}C$ values (Katz et al., 2010), which currently vary between -1‰ and -1‰ (Ravelo & Hillaire-Marcel, 2007).

The $\delta^{13}C$ of seawater DIC can change locally or globally. Local changes are driven by photosynthesis and respiration and changes in upwelling/advection. For example, in areas of high primary productivity, the ^{12}C is preferentially used by organisms during photosynthesis. This process causes the local $\delta^{13}C$ of DIC to shifts towards more positive values. During respiration, oxidation of organic matter release ^{12}C to the water column, resulting in a shift towards more negative $\delta^{13}C$ values. During upwelling, ^{13}C-depleted deep waters can be brought to the surface causing a decrease of surface water DIC $\delta^{13}C$. This reduction in $\delta^{13}C$ values can also occur seasonally as a result of summer stagnation on the open shelf. In coastal regions, humic-rich fluvial or swamp waters can also contribute to change the $\delta^{13}C$ of seawater DIC (Armstrong & Braiser, 2013).

Global changes in the ocean DIC $\delta^{13}C$ are caused by the release (or burial) of carbon from the lithosphere and growth (or decay) of terrestrial biosphere. For example, the $\delta^{13}C$ of DIC can be influenced by volcanic outgassing or gas hydrate dissociation. In addition, because photosynthetic organisms prefer to use ^{12}C during photosynthesis, variation in the size of the terrestrial biosphere can change the ^{13}C content of the atmosphere and ocean (Ravelo & Hillaire-Marcel, 2007).

The $\delta^{13}C$ of planktic foraminifera is influenced by the $\delta^{13}C$ of the surface ocean DIC, but also by "vital" effects, like foraminiferal respiration, presence of symbionts, and calcium carbonate precipitation rates. The foraminiferal respiration and symbiont photosynthesis/respiration influence the "internal carbon pool" microenvironment of the foraminifer, which may vary in pH, DIC concentration, and DIC $\delta^{13}C$ compared to the surrounding seawater. In addition, the precipitation rate of calcium carbonate contributes to the offset between the tests $\delta^{13}C$ and the $\delta^{13}C$ of DIC. Finally, an abiotic kinetic fractionation leads to an enrichment in $\delta^{13}C$ in calcite compared to bicarbonate (HCO_3^-).

The planktic foraminiferal $\delta^{13}C$ can be different among species and among small and large specimens. This can be a consequence of vital effects, changes in habitat preference during the vital cycle, changes in environmental conditions during different seasons, and deposition of a second layer of calcite occurring during sinking of large tests. Finally, diagenesis can also impact the $\delta^{13}C$ of different tests differently (Ravelo & Hillaire-Marcel, 2007).

2.2.5 Oxygen isotopes:

Oxygen has three stable isotopes, ^{16}O, ^{17}O and ^{18}O, and these occur in proportions of 99.76%, 0.04% and 0.2% for ^{16}O, ^{17}O, and ^{18}O, respectively (Bradley, 2015; Pearson, 2012).

The foraminiferal $\delta^{18}O$ reflects the $\delta^{18}O$ of seawater (δ_w) in which the organism calcifies, but it is also a function of the ambient temperature. Because of this, it is possible to use the foraminiferal $\delta^{18}O$ to reconstruct the ocean temperature of the past, when δ_w values are known (Ravelo & Hillaire-Marcel, 2007).

The foraminiferal $\delta^{18}O$ is a function δ_w, which is influenced by global and local processes. The δ_w depends on the global ice volume. The isotope with the highest number of neutrons (^{18}O) is the heaviest, whereas the isotope with the lowest number of neutrons (^{16}O) is the lightest. Because of this, evaporated water is enriched in ^{16}O, whereas the remaining seawater is enriched in ^{18}O. Precipitation is also enriched in ^{18}O compared to water vapor (Bradley, 2015; Pearson, 2012). Thus, clouds forming at lower latitudes and moving polar wards undergo cycles of evaporation and precipitation and contribute to an enrichment in ^{16}O of high latitude snow/ice. (Armstrong & Braiser, 2013; Ravelo & Hillaire-Marcel, 2007). Because of this, during glacial periods ^{16}O is removed from the ocean and trapped in continental ice sheets (Bradley, 2015; Ravelo & Hillaire-Marcel, 2007). Also, during glacial times the temperature is lower. These signals are recorded in foraminiferal tests as more

positive $\delta^{18}O$ values (Armstrong & Braiser, 2013; Bradley, 2015). The opposite happens during interglacial periods.

Local processes, like evaporation/precipitation, melting/growth of sea ice, freshwater input, and advection/upwelling, influence the δ_w, as well (Katz et al., 2010). Evaporation causes an increase in δ_w and surface water salinity because ^{16}O evaporates more easily. During precipitation, the δ_w and surface salinity decreases (Ravelo & Hillaire-Marcel, 2007). At high latitudes, surface waters are influenced by excess precipitation, so these waters have lower $\delta^{18}O$ values. At low latitudes, surface waters are influenced by excess evaporation, so these waters have higher $\delta^{18}O$ values. On a regional scale, the relationship between δ_w and salinity is affected by mixing between regional precipitation (fresh water) and seawater. In the Arctic Ocean, this relationship is complicated by the discharge of large amount of freshwater from rivers, advection, and growth/melting of sea ice. In addition, in the North Atlantic and Arctic the relationship between δ_w and salinity is influenced by meltwater pulses that happened during the deglaciation, when large amount of ^{16}O-rich freshwater was released to the ocean (Bradley, 2015; Ravelo & Hillaire-Marcel, 2007).

In planktic foraminifera, the $\delta^{18}O$ of the test is also influenced by "vital effects". In some species, some of these "vital effects" might be related to the presence of symbionts. In fact, the presence of symbionts might increase calcification rates, which result in lower $\delta^{18}O$ values in adult tests (larger tests). Another complication is represented by the water depth at which the planktic foraminifera live and uncertainties related to the depth preference of foraminifera in the past. The sea surface temperature changes rapidly with depth. Thus, small variations in depth habitat can be equal to a change in water temperature of several degrees Celsius. Thus, it is very important to know which factors control the depth habitat of foraminifera and at which depth the test is secreted (Bradley, 2015; Pearson, 2012).

The carbonate ion (CO_3^{2-}) concentration is another factor that can affect the foraminiferal $\delta^{18}O$ values. When the carbonate ion concentration increases, a decrease in the calcite $\delta^{18}O$ is observed, possibly because the carbonate ion concentration influences the calcification rate and leads to kinetic fractionation effects affecting the incorporation of bicarbonate vs. carbonate ions in calcite. However, further studies are needed to better understand the influence of the carbonate ion (CO_3^{2-}) concentration on the foraminiferal $\delta^{18}O$ (Bradley, 2015; Ravelo & Hillaire-Marcel, 2007).

Planktic foraminifera migrate in the water column during their life. Even though the living foraminifera secrete their test in equilibrium with the upper mixed ocean water, the test of some species becomes enriched in ^{18}O during the process of gametogenesis (reproduction) because of the addition of a layer of gametogenic calcite in deeper waters, which are cooler than surface waters (Bradley, 2015; Ravelo & Hillaire-Marcel, 2007).

Some planktic foraminiferal species are seasonal. Thus, the test $\delta^{18}O$ signature reflects this seasonality (Bradley, 2015; Katz et al., 2010). To be able to use planktic foraminiferal $\delta^{18}O$ as a temperature indicator, it is necessary to establish the influence of temperature, depth, and season on the signal recorded. This can be done by comparing the $\delta^{18}O$ of foraminifera in core-top samples or in sediment traps with the oceanographic conditions of the overlying water column. Culturing studies can also be helpful.

The two last complications when using the planktic foraminiferal $\delta^{18}O$ for paleotemperature reconstructions are dissolution and diagenesis. Dissolution can occur when tests descend down the water column or when they are in the sediment. Dissolution can bias paleotemperature studies because it can dissolve portions of the test that were precipitated before the addition of gametogenic calcite (Pearson, 2012).

Diagenesis also affects the planktic foraminiferal $\delta^{18}O$. Diagenesis can occurs at or near the ocean bottom or deeper in the sediments. Precipitation of diagenetic cements or recrystallization that occur close to the seafloor increases the original foraminiferal $\delta^{18}O$ signature because the temperature at the seafloor is lower compared to the sea surface temperature. Instead, diagenesis that happens deeper in the sediment column (>500m) decreases the original foraminiferal $\delta^{18}O$ signature because of the high sediment temperatures (Armstrong & Braiser, 2013).

2.2.6 Authigenic carbonates on foraminifera tests:

One of the products of AOM coupled with sulphate reduction is the bicarbonate ion. These bicarbonate ions react with calcium (Ca^{2+}) and magnesium (Mg^{2+}) ions that are present in pore waters and precipitate as high-Mg carbonates at the depth of the SMTZ. These carbonates, also called methane-derived authigenic carbonates (MDAC), can occur as secondary overgrowth on foraminiferal tests or as sediment cements (Panieri et al., 2016).

In foraminiferal tests, an enrichment in Mg can indicate the presence of MDAC . Because MDAC are characterized by very low $\delta^{13}C$ values, the very negative $\delta^{13}C$ values that can be

measured in foraminiferal tests from methane seeps can reflect the presence of MDAC on the foraminiferal tests (secondary overgrowth) (Schneider et al., 2017) .

The depth of the SMTZ moves as a consequence of methane flux. During high methane flux, the SMTZ is close to the sediment-water interface, while during low methane flux the SMTZ can be up to tens of meters below the seafloor. At sites of methane seepage, the secondary overgrowth precipitates on foraminiferal tests at the depth of the SMTZ. Thus, if the SMTZ is located near the sea floor, the secondary overgrowth will form roughly at the same time of foraminiferal deposition. In this case, foraminifera with secondary overgrowth would provide a record of methane seepage at the sea floor. If the SMTZ is located several meters below the sediment-water interface, then the secondary overgrowth would be much younger than the foraminiferal test. In this case, the low $\delta^{13}C$ values measured in foraminifera could not be interpreted as a result of methane seepage at the seafloor (Panieri et al., 2016).

3 Materials and Methods:

For this master project, four gravity cores were investigated. These cores were collected in 2013 at Vestnesa Ridge, during a cruise on board the R/V Helmer Hansen on the western margin of Svalbard. After collection, the cores were marked as HH-13-197 (515 cm in length), HH-13-214 (464 cm in length), HH-13-215 (529 cm in length) and HH-13-217 (595 cm in length). The cores were cut into approximately one-meter sections and stored in a cool room during the cruise. At the end of the cruise, these four cores were taken back to The Arctic University of Norway, in Tromsø, where they were frozen until further analysis. Several different methods were used to study these cores (x-ray, magnetic susceptibility, picking of foraminifera, and planktonic foraminiferal stable isotope analysis) in order to reconstruct methane seepage events that occurred during the Pleistocene along the Vestnesa Ridge.

3.1 Seismic survey:

Gas bubbles recorded as flares were first observed at Vestnesa Ridge using echosounder during CAGE cruises with the R/V Helmer Hansen in 2008. Flares were also recorded during cruises in 2010, 2012 and 2013 at Vestnesa Ridge (Mienert et al., 2013; Smith et al., 2014). During the 2013 cruise, methane flares in the water column were detected with the

echosounder mounted on the R/V Helmer Hansen (Kongsberg EK60 multi-frequency echo sounder). Frequencies of 18 kHZ and 38 kHz were used to acquire data. Because of the high impedance between the free gas bubbles and the ocean water, echo sounders are good tools to detect gas bubbles in the water column (Smith et al., 2014). However, the recorded flares might be the result of a single bubble stream or of multi bubble stream. Therefore, recorded flares are not indicative of the amount of methane emitted from the seafloor. The seismic survey provided the possibility to distinguish active (with flares in the water column) from inactive (no flares in the water column) sites and to locate the best position to collect the cores investigated for this master project. Specifically, core GC 19 was collected on the southern side of the ridge, where flares were recorded. The other cores (GC 3, GC 20, GC 22) were taken at locations where no flares were detected, but pockmarks were observed on the ocean bottom.

3.2 Coring:

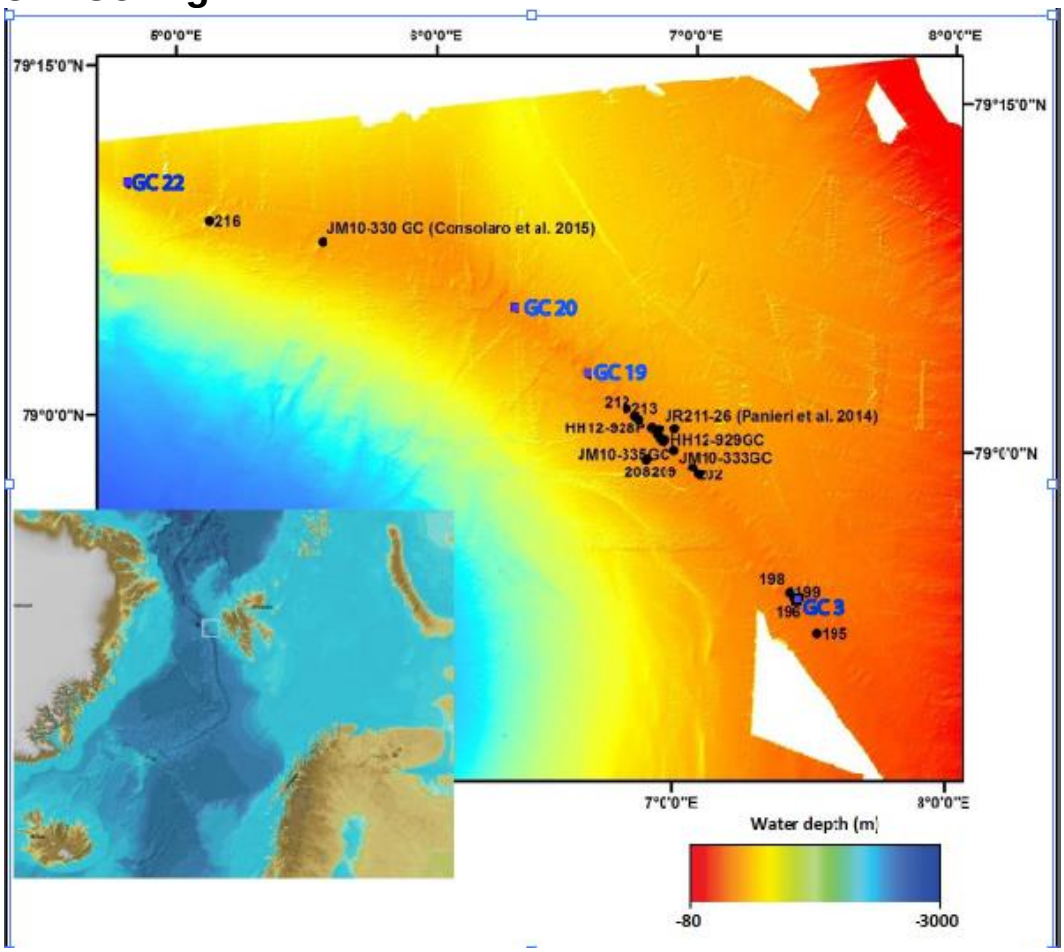

Figure 6 - Overview of the study area and location of several gravity cores collected along Vestnesa Ridge. The 4 different cores studied for this master project are HH-13-197 (GC 3), HH-13-214 (GC 19), HH-13-215 (GC 20), and HH-13-217 (GC 22).

Table 1 – Core ID, core code, site coordinates, year of collection, sediment recovery, depth in meters below sea floor, penetration in cm, seafloor setting, reference, and cruise.

Cores listed by location from SE to NW, coordinates of the cores, year of collection, sediment recovery, depth below seafloor, penetration of gravity corer, seafloor setting of sediments, and cruises.

Core ID + core code	Coordinates	Year	Recovery (cm)	Depth (m bsf)	Penetration (cm)	Seafloor setting	References and cruise
JM03-373PC2	76,240N		837	1485			Jessen et. al. 2010 reference core
	13,060E						
HH-13-197 + GC 3	78,893857N	2013	515	1156,87	659	Pockmark	This study, Cruise CAGE HH-13
	7,441035E						
HH-13-214 + GC 19	79,049027N	2013	464	1211,04	630	Flare only	This study, Cruise CAGE HH-13
	6,6457889E						
HH-13-215 + GC 20	79,093669N	2013	529	1230,96	630	Pockmark	This study, Cruise CAGE HH-13
	6,3577074E						
HH-13-217 + GC22	79,166504N	2013	595	1412,91	590	Pockmark	This study, Cruise CAGE HH-13
	4,8563689E						

The cores studied for this project were taken using a gravity corer. A gravity corer is released down on the seafloor and uses gravity to penetrate it. Weights are placed on the gravity corer for acceleration and to ensure that the corer penetrates the seabed in a straight line, as currents and the vessels movement can influence the accuracy of the coring site position. The gravity corer used allowed to recover up to 6 m of sediment within a PVC tube. A metallic core catcher kept the sediments from escaping. The cores collected were measured, cut into one-meter long sections, labelled, sealed, and frozen.

Core HH-13-197 (GC 3) was taken in the southern part of Vestnesa Ridge (figure 6, table 1). The core was taken within a pockmark and was frozen immediately for further geochemical studies. The cruise report by Mienert et al. (2013) described the core as smelling strongly of hydrogen sulphide. Also, some carbonate crusts were found at the core catcher. Core HH-13-214 (GC 19) was collected from a flare area with no distinct morphology expression on the seafloor, despite a significant flare (figure 6, table 1). Core HH-13-215 (GC 20) was collected in a pockmark without flare. Core HH-13-217 (GC 22) was also collected in a pockmark without flare, but on the northern part of Vestnesa Ridge, where no flare activities have been noted (figure 6, table 1). Flare activities were noted only in the southern part of Vestnesa Ridge.

3.3 Laboratory methods:

The analytical work of this master project was performed at the Department of Geosciences, The Arctic University of Norway, in Tromsø.

3.3.1 X-ray:

The four cores were x-rayed by using a GEOTEK MSCL-XCT x-ray imaging machine. This instrument can take x-rays of whole or open cores. It takes image of 1m sections as the core is

moved through the machine on a conveyor belt. This method is very useful because it allows to see characteristics that would otherwise be difficult to see with a naked eye.

3.3.2 Magnetic susceptibility:

The GEOTEK Multi Sensor Core Logger (MSCL) was used to determine the magnetic susceptibility (MS). The MS is a measurement of how much the sediments are magnetized in relation to a known magnetic field. Magnetic susceptibility, together with sediment lithology, allows to correlate the cores. For this project, the MS was measured on all four cores (GC 3, GC 19, GC 20 and GC 22) and the MS-logs were correlated to the MS-log from Jessen et al. (2010).

3.3.3 Splitting of sediment cores:

All the four cores were split in half, in order to visually study the sediments and take samples. The cores were splitted using a Kawohol sediment liner saw. One half of the core was kept as an archive and stored in a cold room at the Department of Geosciences, The Arctic University of Norway, in Tromsø. The other half was used for sampling purposes. Both halves were labelled with core name and top and bottom, and wrapped in plastic foil to preserve the sediments during storage. When the cores were split, a strong smell of hydrogen sulphide was detected only from core GC 3.

3.3.4 Sampling:

Table 2 – Core ID, core code, sections length, core sections, samples for foraminiferal analysis, and total samples.

Core Identification and core code, the length of the sections, sections dividing the core, samples used for foraminifera analysis, and the total of samples from each section.				
Core ID + core code	Section length (cm)	Sections of the core	Samples for foraminifera analysis	total of samples
HH-13-197 + GC 3	100	1	10	55
	100	2	10	
	100	3	10	
	100	4	10	
	115	5	11	
HH-13-214 + GC 19	100	1	10	49
	100	2	10	
	100	3	10	
	100	4	10	
	56	5	5	
HH-13-215 + GC 20	100	1	10	51
	100	2	10	
	100	3	10	
	100	4	10	
	55	5	5	
	60	6	6	
HH-13-217 + GC 22	100	1	10	60
	100	2	10	
	100	3	10	
	100	4	10	
	100	5	10	
	87	6	8	

The working half of each core was gently smoothed to make it easier to see lamination, colour variation, evidence of bioturbation, and lithology. After this, each core surface was studied and all the differences in core lithology were noted. A lithology log was drawn to note the different lithologies, clasts, IRD, shells, bioturbation, oxidation, and lamination that could be seen at the surface of the core. The Munsell colour map was used to find the correct colour code for the different lithologies. After this, each core was sampled every 10cm from the top of the core to the bottom. The samples were approximately 1 cm thick. In addition, some extra samples were taken where distinctive changes were observed in the cores. All the samples were placed in small plastic bags, where core name, section number, and depth in cm from sea bottom were noted.

3.3.5 Sieving:

Before sieving, each sample was weighed. Then, water was added to help separating grains from clay. Each sample was sieved through three different sieves. The top one captured all grains bigger than 1000µm. The second sieve captured all grains bigger than 100µm. The last sieve captured all grains bigger than 63µm. During the sieving, all the clay was washed away. The three grain sizes were then transferred on a paper filter marked with sample name, core name, and grain size (1000µm, 100µm, 63µm) and put into a drying cabinet at a temperature of 60ºC to dry for 24 hours. Once dry, each granulometric section was weighted again. The dry weight of each grain size was noted and compared to the weight collected before sieving. This allowed to calculate how much of the initial weight was represented by the clay that was washed away. After weighing, each grain size was stored in a plastic bag marked with sample name, core name, and grain size. The three different grain sizes were put together in a paper bag marked with sample name and core name.

3.3.6 Picking for foraminifera:

The foraminiferal picking was performed on all samples from the four different cores included in this study (Table 2). For each sample, foraminifera were picked from the fraction >100µm. Each sample was poured carefully on a picking tray. The tray was then placed under a binocular microscope, so to identify and distinguish individual grains from foraminifera. The tray is divided in 45 squares and these were systematically looked through and studied for foraminifera. The foraminifera were identified, but only one species of planktic foraminifera (*Neogloboquadrina pachyderma s/d*) and one species of benthic foraminifera (*Cassidulina neoteretis*) were picked.

The goal was to pick 20 well-preserved specimens each species, or as many as there were in each of the sample studied. Planktic and benthic foraminifera were placed in separate slides. These slides were marked with core name, sample name, and the name of species. In some of the samples analysed, there were no planktic foraminifera, whereas in others there were no benthic foraminifera. From core GC 3, 51 samples contained planktic foraminifera and 52 samples contained benthic foraminifera. From core GC 19, planktonic foraminifera were picked from 49 samples and benthic foraminifera from 47 samples. From core GC 20, 46 samples contained planktic foraminifera, whereas 43 samples contained benthic foraminifera. From core GC 22, planktonic foraminifera were picked from 61 samples and benthic foraminifera from 50 samples.

This thesis focuses only on planktic foraminifera (*Neogloboquadrina pachyderma*), therefore only these were analysed by mass spectrometry.

3.4 Mass spectrometer analysis:

The carbon and oxygen stable isotope composition ($\delta^{13}C$ and $\delta^{18}O$) of *Neogloboquadrina pachyderma* was determined using a Thermo-Fisher MAT253 IRMS with a Gasbench Ⅱ. Analysis were performed in the Mass Spectrometry Laboratory at The Arctic University of Norway, in Tromsø. From each sample, a minimum of 10-15 specimens were transferred into 4.5ml vials for mass spectrometry analysis. The vials were flushed with He before the manual addition of 5 drops of water free H_3PO_4. After equilibration >3h at a temperature of 50ºC, the samples were analysed. Data were normalized to the Vienna Pee Dee Belemnite by analysis of 2-3 in-house standards with a wide range of $\delta^{13}C$ and $\delta^{18}O$ values. Instrument uncertainty for both $\delta^{13}C$ and $\delta^{18}O$ was $\leq$0.1‰ (standard deviation, Thermo Scientific). For this thesis, the *Neogloboquadrina pachyderma* isotopic composition was analysed in a total of 195 samples.

4 Results:

All four sediment cores object of this master project were visually inspected. Core pictures, x-rays and magnetic susceptibility data (Johnson et al., 2014) were used to compare the cores analysed here with the core results by Jessen et al. (2010), which represents a reference core

of the studied area. This comparison allowed to identify different layers in the studied cores and to place these cores in a stratigraphic context. In addition, the isotopic analysis conducted on planktonic foraminifera as part of this study provided the opportunity to assess past methane seepage activity at the studied site along Vestnesa Ridge.

4.1 Core description:

Core HH-13-197, GC 3:

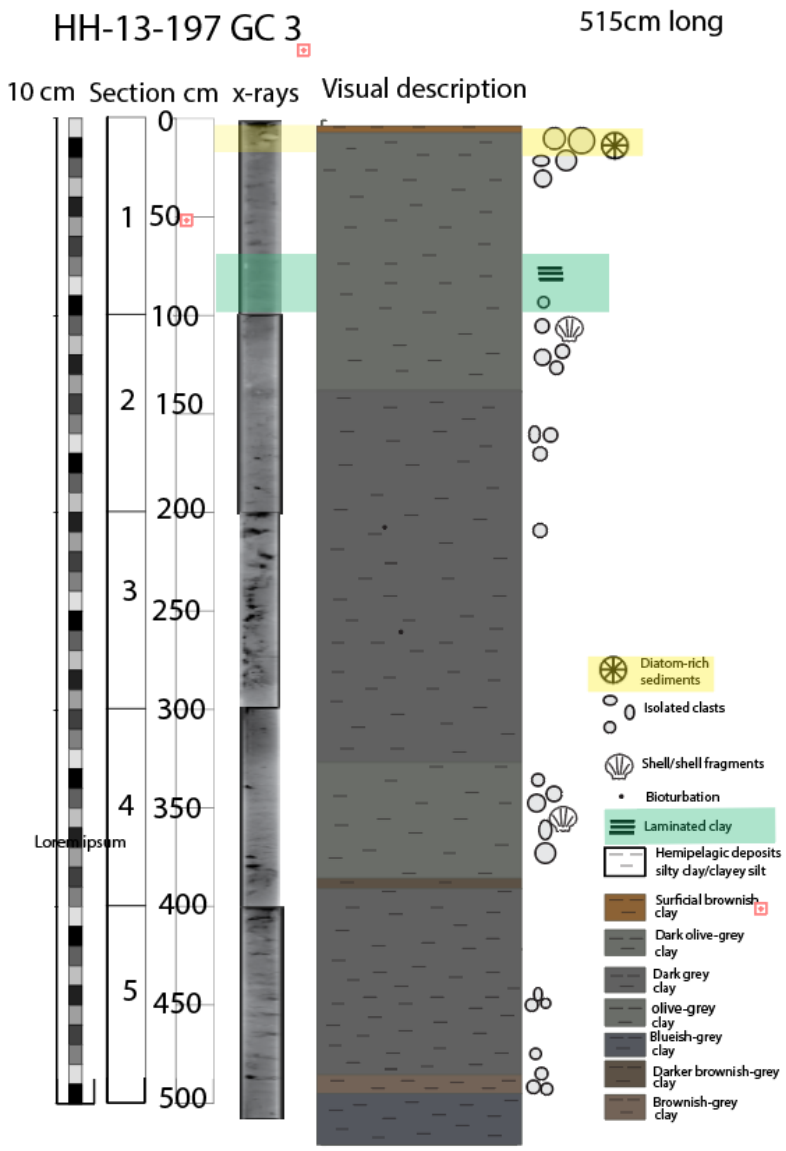

Figure 72 – Core GC 3 visual description with lithology and x-ray images.

The core GC 3 consist of mostly dark grey clay with some layers of olive grey clay and brownish clay in between. There are several layers within the core that are rich in Ice Rafted Debris (IRD) and shell fragments. These layers may have been deposited during colder

periods, when Vestnesa Ridge was covered by ice. From 5-15cm is there is a layer consisting of brownish grey very fine-grained clay with pebbles and diatoms. Around the depth of 70cm to 100cm is a layer consisting of laminated clay (figure 7). There is little bioturbation in the core. The x-rays show centimetric intervals of disturbed sediments, this may be gas bubbles.

Core HH-13-214, GC 19:

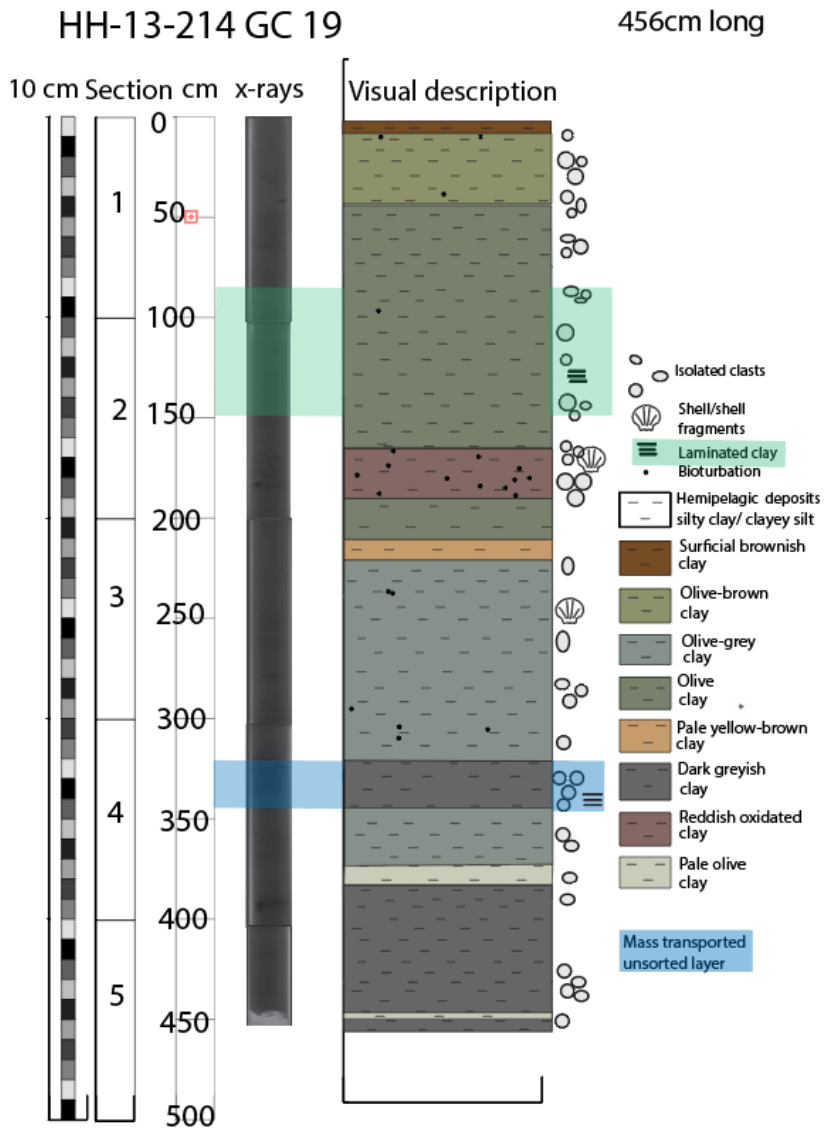

Figure 8 – Core GC 19 visual description with lithology and x-ray images.

Core GC 19 consists of mostly olive, grey and dark greyish layers of clay/silty clay. It has been observed the presence of centimetric pebbles, some shell fragments and traces of bioturbation. A layer of reddish colour clay at the interval 166-186cm contains abundant bioturbation. At a depth of 84cm and down to 148cm is there an 64cm thick laminated layer

(figure 8). The x-ray photos show clearly the lamination. There is an unsorted layer at a depth of 325cm to 356cm, this layer is 31cm thick and consists of mostly dark greyish clay with pebbles and cobbles. Very weak lamination have been observed within this layer.

Core HH-13-215, GC 20:

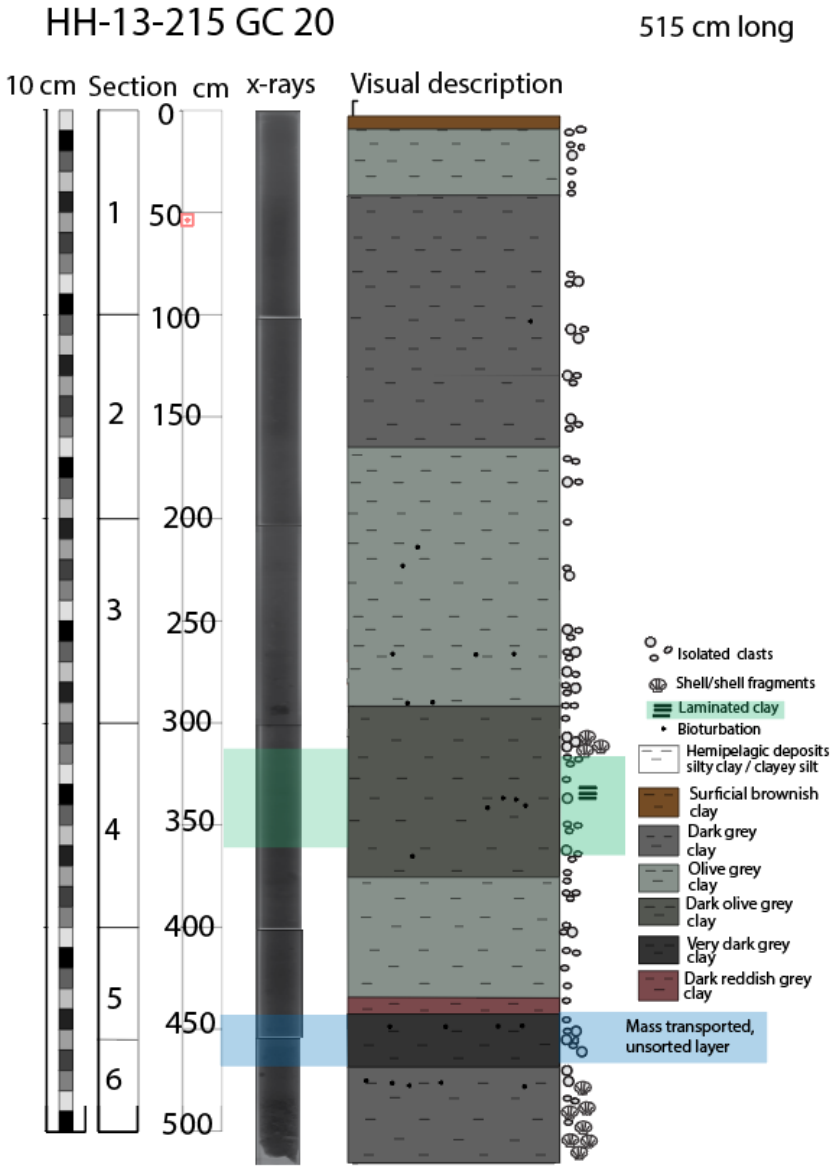

Figure 9 – Core GC 20 visual description with lithology and x-ray images.

Core GC 20 consists mainly of dark grey layers of silty clay with some olive grey layers. In this core traces of bioturbation are visible especially from the middle to the bottom of the core. There are slightly more abundant pebbles and shell fragments from the middle to the bottom part of the core. From 315 to 360cm there is a 45cm thick layer with laminated dark

grey, which was observed also in the x-ray images (figure 9). There is an unsorted layer of very dark clay with lots of pebbles at a depth of 440cm and continuing to 465cm. At the very bottom of the core there is a layer consisting of mostly shell fragments.

Core HH-13-217, GC 22:

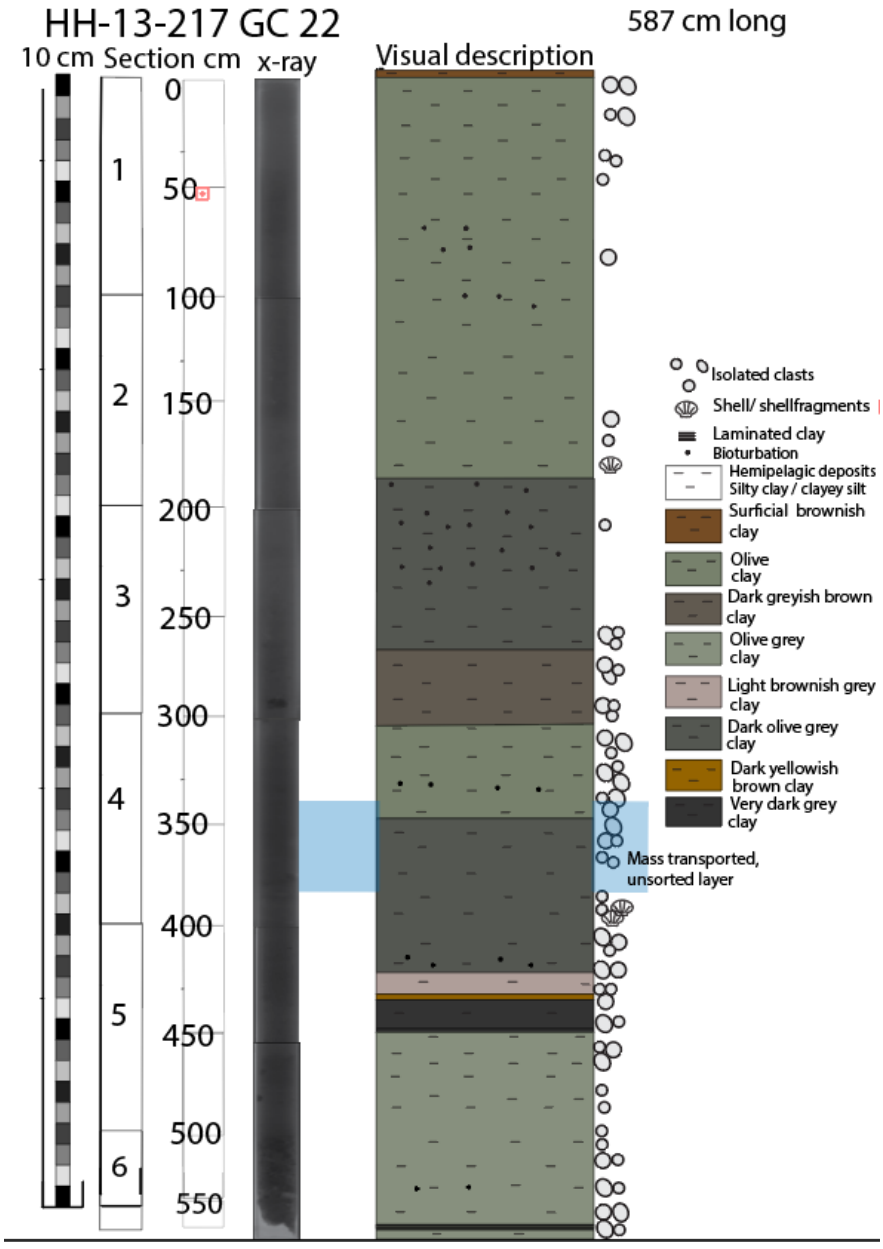

Figure 10 – Core GC 22 visual description with lithology and x-ray images.

Core GC 22 consists of olive silty clay layers with two darker olive/brownish layers in the middle part of the core. The core shows evidence of bioturbation, especially in the middle part of the core. Like in the other cores, some pebbled are present, mostly toward the top of the

core. The lower half however, contains a lot of pebbles and some shell fragments. Around 340cm depth is a dark unsorted layer found which ends at about 385cm depth (figure 10).

4.2 Magnetic susceptibility:

The magnetic susceptibility (MS) obtained from the studied cores have been correlated with those obtained measuring sediment cores collected on the western Svalbard slope from Jessen et al. (2010). The general trend of the MS from two of the here investigated cores is in accordance to Jessen et al. (2010). In the studied cores, the MS exhibits two intervals with low values. Both of these lower values intervals are observed in core GC 19, while in core GC 22 is only the oldest of the two low intervals observed (figure 12 and 14). On the contrary, the magnetic susceptibility data for core GC 3 and GC 20 is very low or erased which is indictive of sediments influenced by methane seepage were the iron-oxides like ferromagnetic magnetite (Fe_3O_4) exposed to hydrogen-sulphide produced by AOM (figure 11 and 13). This process leads to a reduction to paramagnetic pyrite (FeS_2) which causes a low in the MS signals (Schneider et al., 2018).

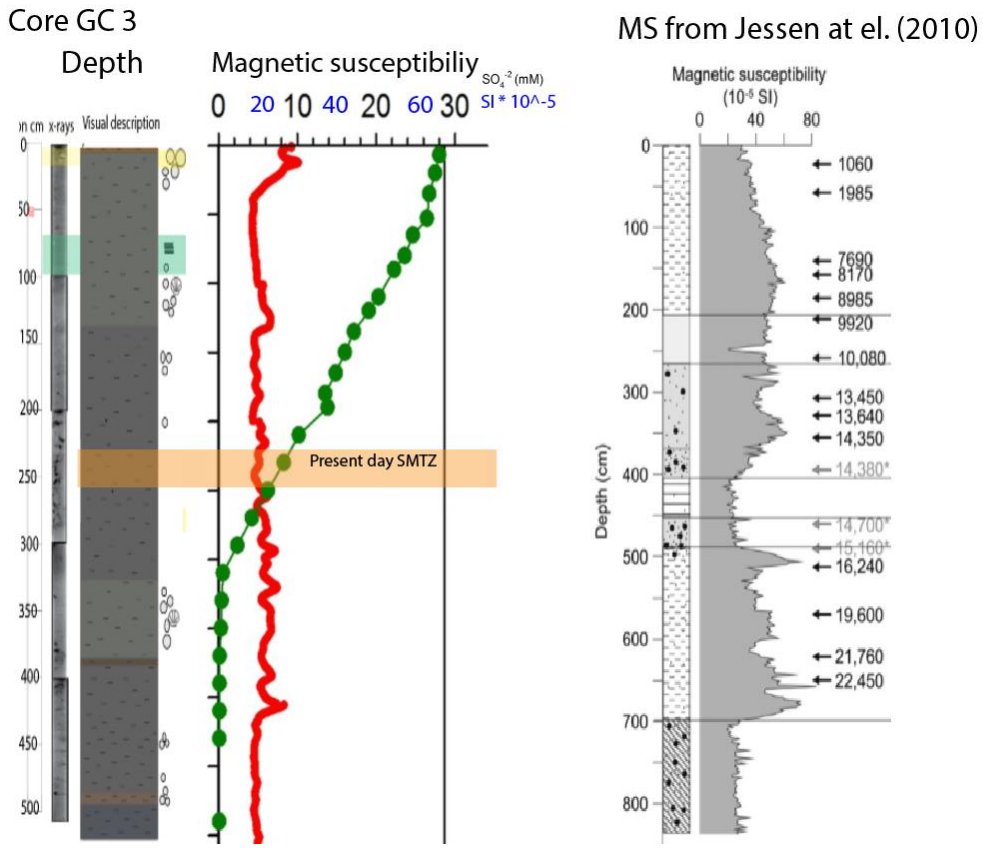

Figure 11 – Core GC 3, lithology together with MS record, and MS record from Jessen et al. (2010). The green dotted green line reflects sulphate content measured in the pore water. This is the only core in this study which has been analysed for sulphate in the pore water.

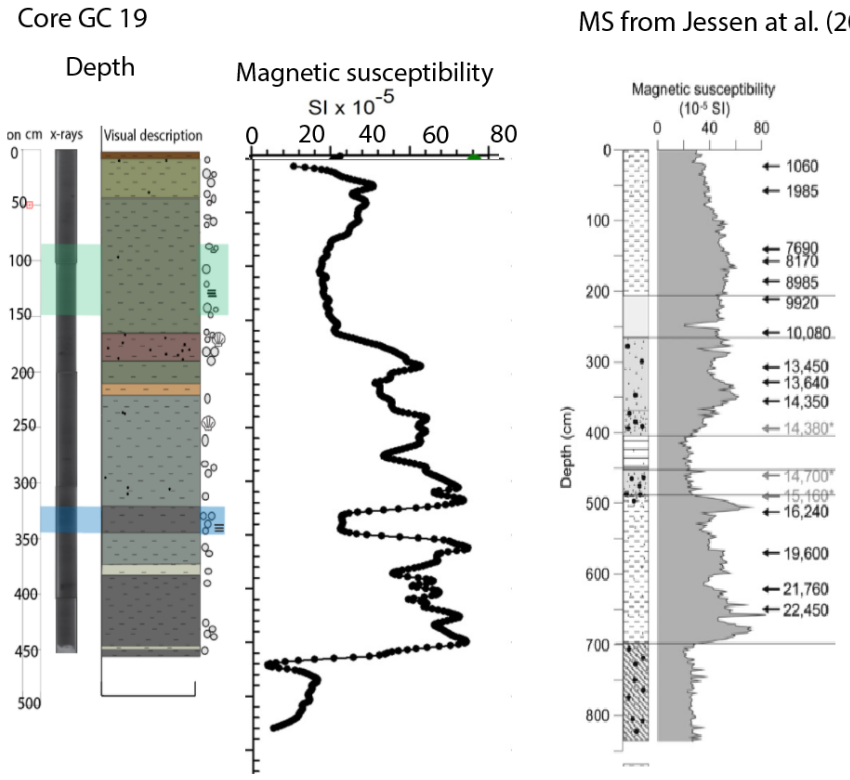

Figure 12 – Core GC 19, lithology together with MS record, MS record from Jessen at el. (2010).

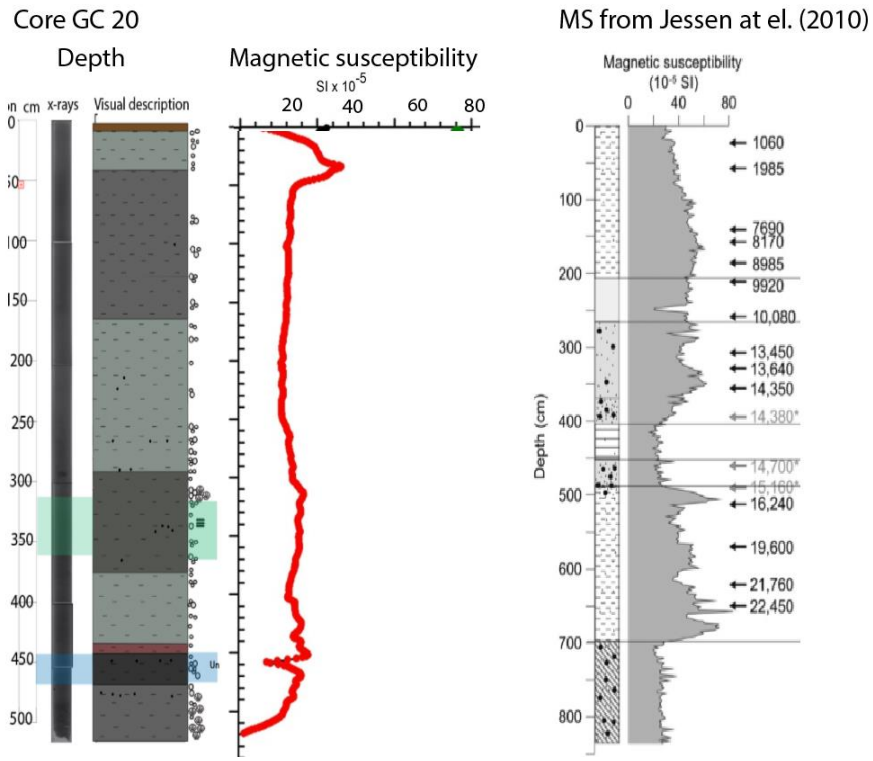

Figure 33 – Core GC 20, lithology together with MS record, and MS record from Jessen et al. (2010).

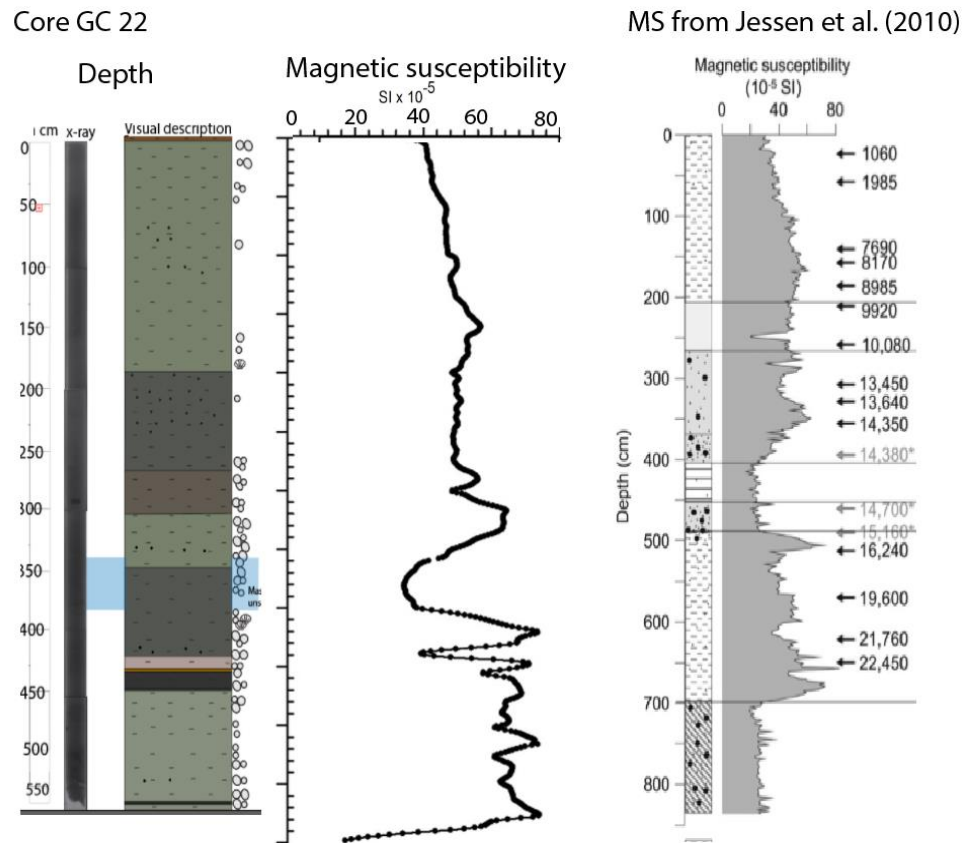

Figure 44 – Core GC 22, lithology together with MS record, and MS from Jessen et al. (2010).

4.3 State of preservation of foraminifera shells:

The samples analysed for foraminifera were characterized by variation in abundance of specimens of both benthic and planktonic foraminifera: some contained high abundances while others contained low abundances of foraminifera tests. Some of the foraminifera tests were all white and in a very good condition, some were more transparent or yellowish and some were greyish, broken and in a very bad condition (see tables 3-6 where there are the original observations made during the picking of foraminifera for isotopic analyses). The foraminifera tests with very good preservation condition are pristine, and these are not impacted by diagenetic alteration. There are no foreign grains or crystals on the exterior tests and they seem to resemble the living modern foraminifera tests. For the isotope analysis, the best preserved tests of the planktic foraminifera *Neogloboquadrina pachyderma* were selected.

Core CG 3 and GC 20 contained foraminifera tests that generally were in poorer condition than Core GC 19, and GC 22 (tables 3-6). From these cores, also tests of the planktic foraminifera *Neogloboquadrina pachyderma* that present moderate diagenetic alterations or have badly preserved tests were chosen for isotopic analyses.

HH-13-197 GC3		Foraminifera (counting and color)			Isotop anaysis result	
		Planktic foraminifera			N. pachyderma	
samples dept	sectic	N. pachyderma		Description	d13C VPDB [‰	d18O VPSB [‰]
0-1cm	1	23	white	Not so many forams, good condition	-0,25	2,70
10-11cm	1	24	white, grey/yellow	Some forams, but not many. Good condition	-0,01	2,87
20-21cm	1	21	white, grey/yellow	Not that many forams, good condition	-0,23	4,04
30-31cm	1	21	white, grey/yellow	Few forams, espesially planktic, good condition	-0,52	4,05
40-41cm	1	21	white, grey/yellow	Few forams, espesially benthic, good condition		
50-51cm	1	4	white	Very few forams, some broken.		
60-61cm	1	11	white	Few forams, some broken.	-0,88	3,79
70-71cm	1	26	white	Few benthic, many planktic forams. Some broken.	-1,59	4,44
80-81cm	1	9	white	Few forams, some broken.		
90-91cm	1	1	a bit grey	Many benthic, 1 planktic forams. Good condition		
100-101cm	2	0		Only benthic forams, good condition		
110-111cm	2	25	white, grey/yellow	Many benthic, few planktic forams. Bad con.	-8,72	4,28
120-121cm	2	21	white, grey/yellow	Many benthic, very few planktic. Good condition	-3,93	4,25
130-131cm	2	24	white, grey/yellow	Many forams. Good condition.	-2,18	3,73
140-141cm	2	27	white, grey/yellow	Many forams. Good condition.	-1,21	2,77
150-151cm	2	26	white, grey/yellow	Many forams. Good condition.	-1,01	3,58
160-161cm	2	20	white, grey/yellow	Many forams. Good condition.	-1,38	4,69
170-171cm	2	45	white, grey/yellow	A lot of forams, espesially planktic. Good condition.	-0,63	4,56
180-181cm	2	38	white, grey/yellow	A lot of forams, espesially planktic. Good condition.	-0,81	4,76
190-191cm	2	44	white, grey/yellow	Many forams, espesially planktic. Good condition	-1,72	4,71
200-201cm	3	35	white, grey/yellow	Many forams, espesially planktic. Good condition	-1,33	4,67
210-211cm	3	36	white, grey/yellow	Many forams, espesially planktic. Good condition	-1,26	4,73
220-221cm	3	70	white, grey/yellow	Many planktic forams, few benthic. Some broken	-0,83	4,68
230-231cm	3	34	white, grey/yellow	Many forams, espesially planktic. Good condition	-0,62	4,61
240-241cm	3	32	white, grey/yellow	Many forams, espesially planktic. Good condition	-1,46	4,66
250-251cm	3	22	white, grey/yellow	Many forams, espesially planktic. Good condition	-0,64	4,62
260-261cm	3	22	white, grey/yellow	Many forams. Good condition	-1,01	4,77
270-271cm	3	40	white, grey/yellow	Very many planktic, few benthic forams. Good con.	-0,69	4,79
280-281cm	3	42	white, grey/yellow	Many forams, espesially planktic. Good condition	-0,54	4,77
290-291cm	3	26	white, grey/yellow	Very many planktic, few benthic forams. Good con.	-0,60	4,71
300-301cm	4	32	white	A lot of planktic, fewer benthic forams. Good con.	-0,69	4,75
310-311cm	4	25	white, grey/yellow	Many benthic, fewer planktic forams. Good con.	-0,92	4,69
320-321cm	4	28	white, grey/yellow	Many planktic, fewer benthic forams. Good con.	-1,00	4,73
330-331cm	4	26	white, grey/yellow	Very few forams, lots of broken ones.	-5,99	4,74
340-341cm	4	21	white, grey/yellow	Very few forams. Not a good condition	-1,33	4,31
350-351cm	4	7	white, grey/yellow	Few forams. Not a good condition (grey crystals)		
360-361cm	4	18	white, grey/yellow	Few forams. Not a good con. (grey crystals)	-4,34	4,66
370-371cm	4	2	white, grey/yellow	Few forams. Not a good condition		
380-381cm	4	24	white, grey/yellow	Lots of forams. Ok condition.	-0,71	4,61
390-391cm	4	25	white, grey/yellow	Very many forams. Bad condition.	-1,03	4,51
400-401cm	4	27	white, grey/yellow	Many planktic, fewer benthic forams. Good con.	-0,49	4,44
					-0,25	4,24
408-409cm	5	40	white, grey/yellow	Nearly only planktic forams. Ok condition	-0,39	4,24
418-419cm	5	30	white, grey/yellow	Not many forams, many broken ones. Not good con.	-0,46	4,24
428-429cm	5	24	white, grey/yellow	Many forams, good condition.	-0,72	4,24
438-339cm	5	31	white, grey/yellow	A lot of forams, espesially planktic. Good con.	-1,06	4,24
448-449cm	5	28	white, grey/yellow	A lot of forams, espesially planktic. Good con.	-3,66	4,24
458-459cm	5	28	white, grey/yellow	A lot of forams, good con.	-2,36	4,24
468-469cm	5	20	white, grey/yellow	Fewer forams, espesially benthic.	-3,28	4,24
478-479cm	5	16	white, grey/yellow	Very few forams, espesially benthic. ok condition.	-0,44	4,24
488-489cm	5	21	white, grey/yellow	Many forams. Some broken, bad con. (grey crystals)	-5,30	4,24
498-499cm	5	18	white	Few forams, espesially benthic. Good condtion	-4,07	4,24
505-506cm	5	28	white, grey/yellow	Few forams, espesially benthic. Good condtion	-1,35	4,24
514-515cm	5	20	white, grey/yellow	Few forams, espesially benthic. ok condtion	-0,11	4,24
423-424cm	5	11	grey, yellow, white	Bad condition, lots of brownish spots.		
446-447cm	5	26	white, yellow/grey	Moderate condition.	-1,48	4,24

Table 3 – Core GC 3 samples and foraminifera picked, their condition, and isotope results ($\delta^{13}C$ and $\delta^{18}O$). A complete table is provided as an attachement at the end of this thesis.

HH-13-214 GC19		Foraminifera (counting and color)		Isotop anaysis result	
		Planktic foraminifera		Planktic	
sample depl	section	N. pachyderma	Description	N. pachyderma	
1-2	1	25 white	few forams, moderate condition some holes	d13C VPDB [%	d18O VPSB [%]
11-12		24 white	moderate condition some holes	0,15	2,92
21-22		14 white	small sample, moderate-better condition	0,19	3,26
31-32		22 white	small sample, moderate-better condition	-0,03	3,31
41-42		24 white	moderate condition some holes	-0,49	4,03
51-52		22 white	moderate condition some holes	-0,17	4,17
61-62		27 yellow/white	many forams, moderate condition some holes	-0,18	4,09
71-72		18 yellow/white	small sample, moderate condition	-0,03	4,09
81-82		30 yellow/white	small sample many forams, moderate condition	-0,31	4,32
91-92		27 white	very small sample many forams, moderate condition	-0,44	4,09
101-102	2	27 white	very small sample many forams, moderate condition	-0,39	4,21
111-112		4 white	very small sample few forams, moderate condition	-0,27	4,20
121-122		35 white	very small sample many forams, better-moderate condition		
131-132		4 white	few forams, moderate condition	-0,59	4,14
141-142		27 white	many forams, moderate condition		
151-152		27 white	moderate-better condition	-0,23	4,40
161-162		24 white	moderate condition some holes	-0,56	4,16
171-172		22 white	moderate condition some holes	-0,13	4,43
181-182		28 white	moderate condition some holes	-0,27	4,18
191-192		22 grey/white	many forams, bad condition many gray ones	-0,16	3,86
201-202	3	28 white	many forams, moderate-better condition	-0,26	2,62
211-212		25 white	many forams, moderate-better condition	-0,10	4,75
221-222		24 white	many forams, moderate-better condition	-0,33	3,41
231-232		26 white	many forams, moderate condition	-0,02	4,90
241-242		24 white/grey	many forams, moderate condition	0,00	4,68
251-252		29 white	many forams, moderate-better condition	0,00	4,83
261-262		24 white	many forams, moderate-better condition	-0,27	4,55
271-272		25 white	many forams, moderate-better condition	0,04	4,88
281-282		26 white	many forams, moderate-better condition	-0,22	4,64
291-292		26 white	many forams, moderate-better condition	-0,05	4,67
301-302	4	25 white/grey	many forams, moderate condition	0,09	4,84
311-312		23 white/grey	many forams, moderate condition	-0,05	4,58
321-322		8 white	few forams big sample, moderate condition	-0,09	4,76
331-332		2 white	very few forams big sample, moderate condition		
341-342		25 white	moderate condition		
351-352		27 white	many forams, moderate condition	-0,10	4,71
361-362		30 white	many forams small sample, moderate condition	-0,11	4,46
371-372		24 white	many forams very small sample, moderate condition	-0,08	4,11
381-382		17 white/grey	few forams, moderate condition	-0,09	4,52
391-392		23 white/grey	many forams small sample, moderate condition	0,06	4,31
401-402	5	24 white/grey	many forams, moderate condition	-0,03	4,59
411-412		25 white	many forams, moderate-better condition	-0,38	4,27
421-422		23 white/yellow	many forams, moderate-better condition	0,08	4,28
431-432		23 white	moderate-better condition	-0,38	4,06
441-442		25 white	moderate condition some holes	0,04	4,49
451-452		33 white/grey	many forams, moderate condition	-0,12	4,38
				0,08	4,15

Table 4 – Core GC 19 samples and foraminifera picked, their condition, and isotope results ($\delta^{13}C$ and $\delta^{18}O$). A complete table is provided as an attachement at the end of this thesis.

HH-13-215 GC20		Foraminifera (counting and color)		Isotop anaysis result	
		Planktic foraminifera		N. pachyderma	
sample dept	sectio	N. pachyderma	Description	d13C VPDB [	d18O VPDB [‰]
1-2	1	29 white	moderate condition	0,23	2,95
11-12		25 white/grey/yellow	moderate condition	0,31	3,28
21-22		30 white/grey/yellow	moderate condition	0,33	2,99
31-32		37 white/grey/yellow	moderate condition	0,48	3,33
41-42		28 white/grey/yellow	small sample, moderate condition	0,57	3,63
51-52		2 white	very few forams small sample, moderate condition		
61-62			small sample		
71-72			small sample		
81-82		27 white/yellow	moderate condition	0,17	4,28
91-92			small sample		
101-102	2		small sample		
111-112			small sample		
121-122		20 white	moderate condition some holes	0,16	3,55
131-132		17 white	moderate condition some holes	0,33	3,55
141-142		3 white	very few forams small sample, moderate-bad condition some holes		
151-152		38 white/yellow/grey	many forams, moderate-better condition	0,03	3,55
161-162		31 white	many forams, moderate condition some broken ones	0,03	3,55
171-172		26 white/yellow/grey	many forams, moderate condition some broken ones	0,03	3,55
181-182		25 white/grey/yellow	many forams, moderate condition some broken ones	0,03	3,55
191-192		25 white/grey/yellow	many forams, moderate condition some broken ones	0,03	3,55
201-202	3	25 white	many forams, moderate condition some broken ones	0,03	3,55
211-212		27 white/grey/yellow	many forams, moderate condition some broken ones	0,03	3,55
221-222		26 white/yellow/grey	many forams, moderate condition some broken ones	0,03	3,55
231-232		23 white/yellow/grey	many forams, moderate condition	-0,03	3,20
241-242		28 white/grey/yellow	many forams, moderate condition	0,10	3,52
251-252		23 white/yellow/grey	few forams, moderate condition	-1,49	3,83
261-262		29 white/yellow/grey	moderate condition	-0,48	3,75
271-272		22 white/yellow/grey	few forams, moderate condition	-0,03	4,10
281-282		27 white/yellow/grey	many forams, moderate condition	-2,51	4,08
291-292		22 white/yellow/grey	few forams, moderate condition some broken	-0,17	3,31
301-302	4	26 white/yellow/grey	few forams, moderate condition some broken	-0,74	4,29
311-312		24 white/yellow/grey	few forams, moderate condition some broken	-0,07	4,42
321-322		10 white/yellow/grey	few forams, moderate condition some broken	-0,14	3,89
331-332		24 white/yellow/grey	bad condition (grey crystals)	-13,13	5,03
341-342		7 white/yellow/grey	few forams, bad condition some broken (grey crystals)		
351-352		28 white/grey/yellow	many forams small sample, moderate-bad condition	-4,25	4,85
361-362		29 white/yellow/grey	many forams, moderate condition	-3,41	4,63
371-372		24 white/yellow/grey	moderate condition	-0,32	4,46
381-382		28 white/grey/yellow	moderate condition	-2,72	4,41
391-392		40 white/grey/yellow	many forams small sample, moderate condition	-0,33	3,82
401-402	5	28 white/grey/yellow	many forams, moderate condition	-0,43	2,83
411-412		27 white/grey/yellow	many forams, moderate condition	-3,97	4,80
421-422		23 white/yellow/grey	many forams, moderate condition	-2,95	4,38
431-432		26 white/yellow/grey	many forams, moderate condition	-4,63	4,81
441-442		26 white/yellow/grey	many forams, moderate condition	-2,20	4,32
451-452		34 white/yellow/grey	many forams, moderate condition	-0,90	4,65
461-462		26 white/yellow/grey	moderate condition	-1,42	4,67
471-472		29 white/yellow/grey	moderate condition	-2,21	4,35
481-482		35 white/yellow/grey	many forams, moderate condition	-0,14	4,70
491-492		31 white/yellow/grey	many forams, moderate condition	-2,93	4,67
501-502	6	29 white/yellow/grey	moderate-bad condition	-8,98	5,29

Table 5 – Core GC 20 samples and foraminifera picked, their condition, and isotope results ($\delta^{13}C$ and $\delta^{18}O$). A complete table is provided as an attachement at the end of this thesis.

HH-13-217 GC22		Foraminifera (counting and color)		Isotop analysis results	
		Planktic foraminifera		N. pachyderma	
sample depth	section	N. pachyderma	Description	d13C VPDB [‰]	d18O VPDB [‰]
1-2	1	27 white/grey	many forams very small sample, moderate cond	0,36	3,39
11-12		29 white	moderate condition	0,43	3,26
21-22		32 white	moderate condition some holes	0,34	3,41
31-32		39 white/grey	many forams, moderate condition	0,20	3,30
41-42		25 white	many forams, moderate condition	0,74	3,50
51-52		30 white	many forams, moderate condition some holes	0,77	3,55
61-62		30 white	many forams, moderate condition some holes	0,63	3,47
71-72		33 white	many forams, moderate-better condition	0,69	3,64
81-82		25 white	many forams, moderate-better condition	0,40	3,20
91-92		24 white/yellow	many forams, moderate condition	0,63	3,36
101-102	2	24 yellow/white	moderate-better condition	0,45	3,55
111-112		22 white/grey	many forams, moderate condition	0,46	3,23
121-122		24 white	many forams, moderate-better condition	0,48	3,29
131-132		30 white	many forams, moderate condition	0,39	3,14
141-142		27 white	many forams, moderate condition	0,55	3,14
151-152		27 white	many forams, moderate condition	0,27	3,05
161-162		22 white	moderate condition	0,31	2,83
171-172		33 white/grey	moderate condition	0,12	3,03
181-182		31 white	moderate condition	0,20	4,03
191-192		22 white	many forams, moderate condition	0,01	2,96
201-202	3	22 white	moderate condition	-0,04	3,02
211-212		28 white	many forams, moderate condition	-0,23	2,93
221-222		24 white	many forams, moderate condition	-0,05	3,16
231-232		22 white	many forams, moderate condition	-0,05	3,25
241-242		22 white	many forams, moderate condition	0,09	3,49
251-252		28 white	many forams, moderate condition	0,12	3,74
261-262		22 white/yellow	moderate condition	0,10	3,58
271-272		27 white	many forams, moderate condition	0,04	3,87
281-282		25 white/grey	many forams, moderate condition	0,12	3,18
291-292		2 white	very few forams small sample, moderate condition		
301-302	4	33 white/yellow	many forams small sample, moderate condition	-0,16	4,49
311-312		23 white	small sample, moderate condition	-0,12	4,27
321-322		25 white	moderate-better condition	0,09	4,14
331-332		28 white	many forams, moderate condition	-0,07	4,24
341-342		24 white/grey	moderate condition	-0,03	4,24
351-352		24 white	moderate condition	-0,09	4,49
361-362		14 white	small sample, moderate condition some holes	-0,23	4,36
371-372		23 yellow	small sample, moderate condition some holes	-0,27	4,28
381-382		22 white	small sample, moderate condition some holes	-0,35	4,33
391-392		30 white	moderate condition	-0,08	4,66
401-402	5	52 white	moderate-better condition	-0,06	4,53
411-412		28 white	moderate-better condition	-0,10	4,53
421-422		23 white	moderate-better condition	-0,10	4,81
431-432		25 white	moderate condition	-0,10	4,72
441-442		25 white	moderate condition	-0,17	4,46
451-452		5 white	moderate condition		
461-462		25 white	moderate condition	0,02	4,17
471-472		25 white/yellow	moderate condition	0,01	4,26
481-482		1 white	moderate condition		
491-492		50 white	moderate condition	0,11	4,60
501-502	6	15 yellow/grey	moderate condition	-0,16	4,83
511-512		21 yellow/grey	moderate condition	-0,11	4,63
521-522		23 grey/yellow	moderate condition some holes	0,00	4,54
531-532		25 grey/yellow	moderate-bad condition some holes	-0,02	4,68
541-542		24 white/yellow	moderate condition	0,34	4,55
551-552		20 white/yellow	moderate condition	0,19	4,53
561-562		16 white/yellow	moderate condition	-0,11	4,15
571-572		21 grey/white	moderate-bad condition	0,14	4,38
581-582		25 white/yellow/grey	moderate condition	0,17	4,47

Table 6 – Core GC 22 samples and foraminifera picked, their condition, and isotope results ($\delta^{13}C$ and $\delta^{18}O$). A complete table is provided as an attachement at the end of this thesis.

4.3.1 Isotope measurements:

The results from the isotope analysis of *Neogloboquedrina pachyderma* from the four cores gives both the $\delta^{13}C$ and $\delta^{18}O$. The $\delta^{13}C$ and $\delta^{18}O$ is expressed as Vienna Pee Dee Belemnite VPDB to allow for comparison with published datasets. The result of the foraminiferal isotope analysis are summarized in figures 15-18. In these figures, the isotope data are plotted together with the core description.

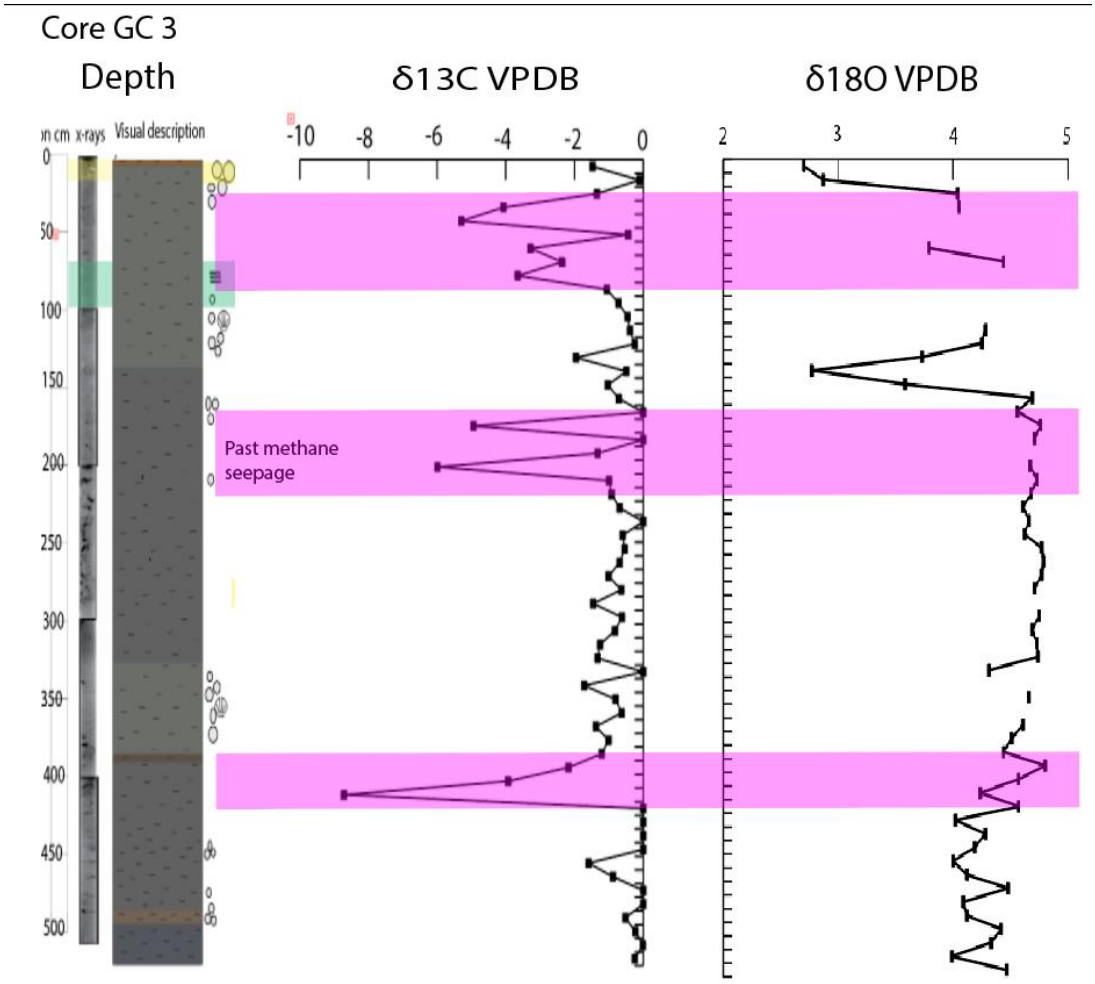

Figure 15 – Core GC 3 lithology, $\delta^{13}C$ and $\delta^{18}O$ isotope signals. The pink bars represent the reconstructed past methane emission events.

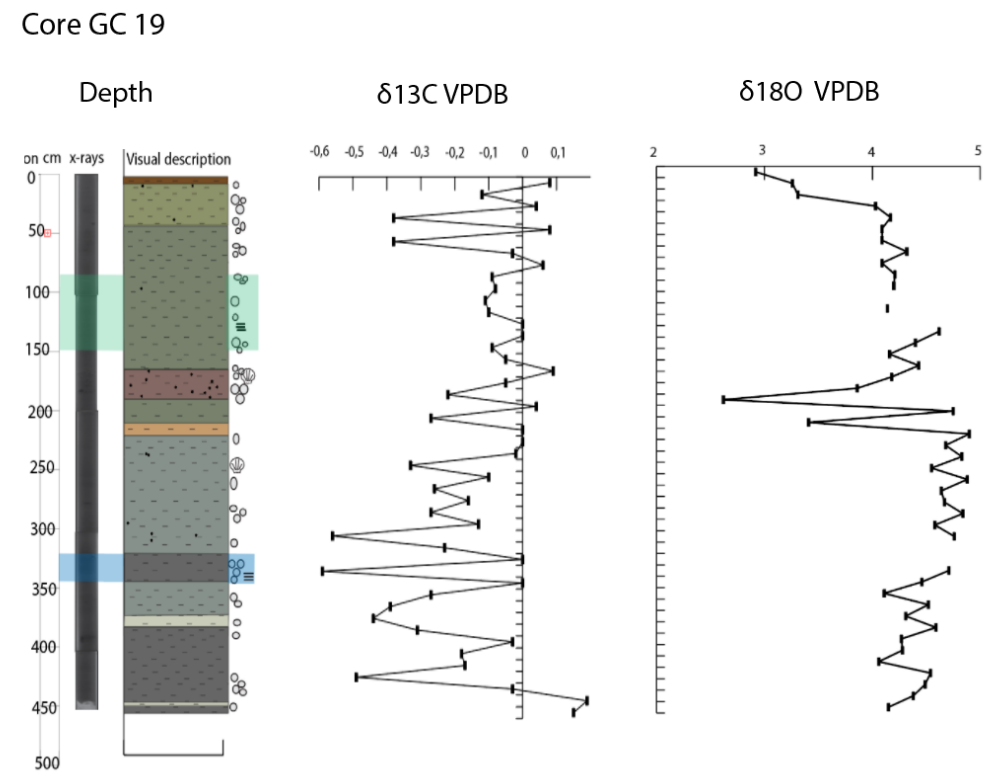

Figure 16 – Core GC 19 lithology, $\delta^{13}C$ and $\delta^{18}O$ isotope signals.

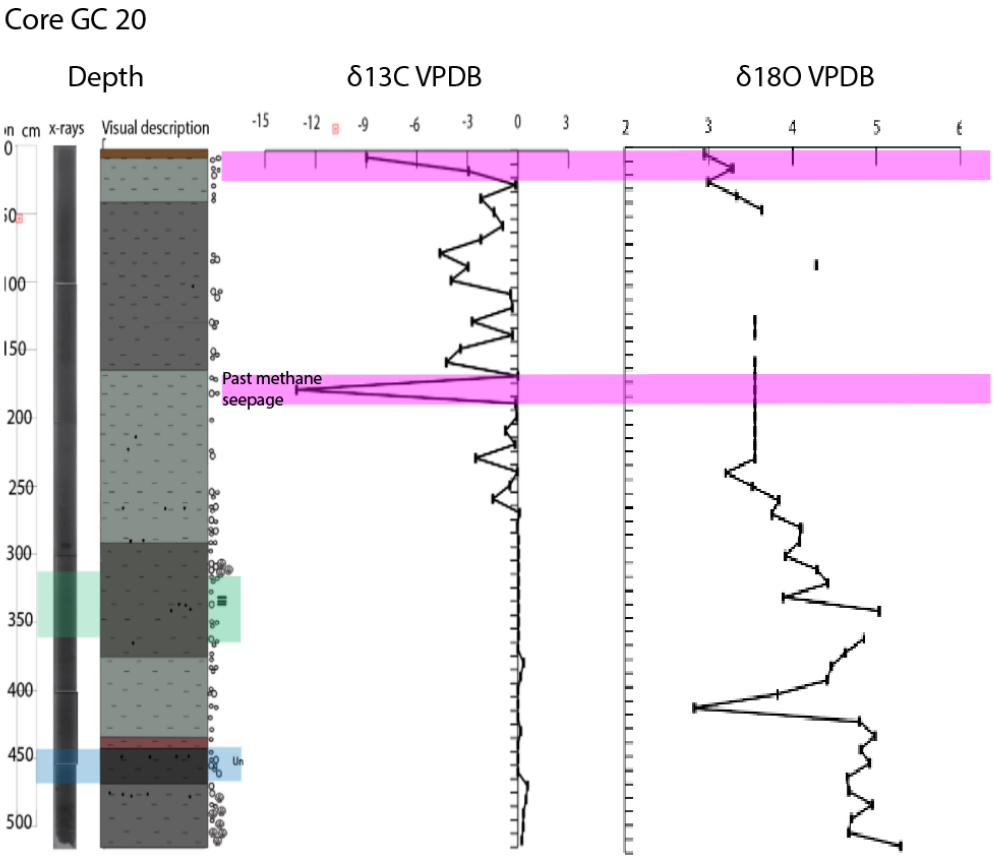

Figure 17 – Core GC 20 lithology, $\delta^{13}C$ and $\delta^{18}O$ isotope signals. The pink bars represent the reconstructed past methane emission events.

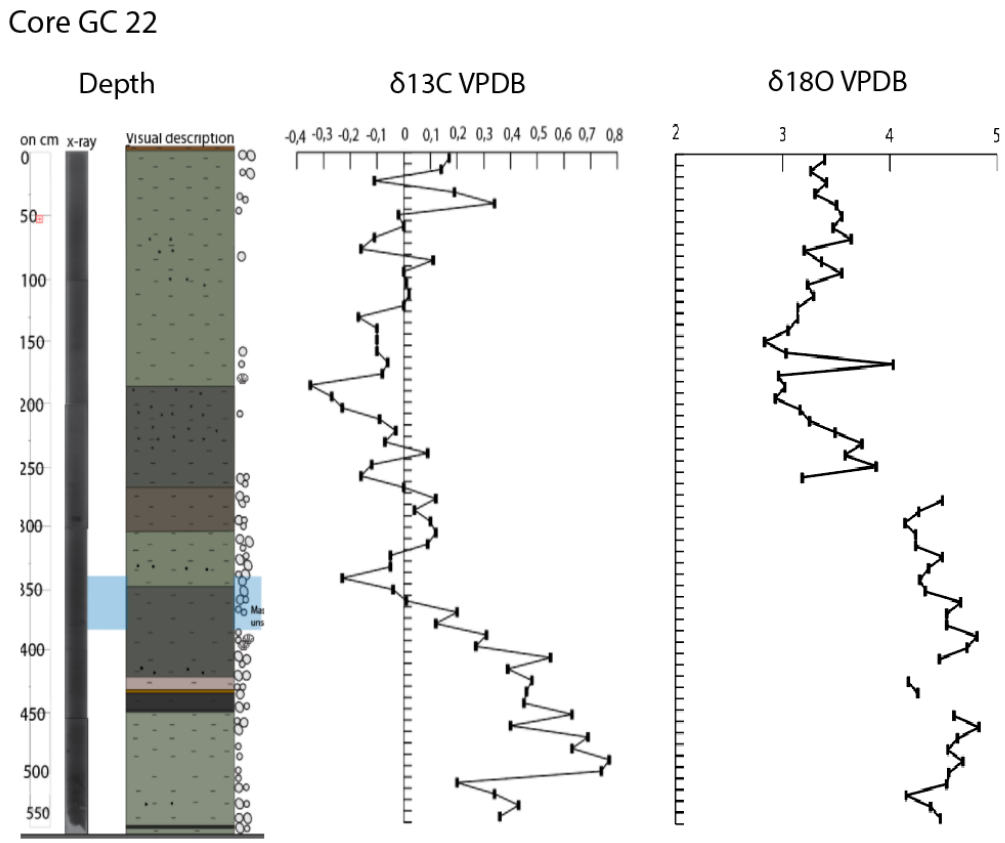

Figure 18 – Core GC 22 lithology, $\delta^{13}C$ and $\delta^{18}O$ isotope signals.

4.3.2 $\delta^{13}C$ isotope values:

The $\delta^{13}C$ data ranges from 1‰ to -15‰. Core GC 3 is characterized by $\delta^{13}C$ values as negative as -10‰, whereas values from core GC 20 recorded negative values to nearly -15‰ (tables 3 and 5, figures 15 and 17). Cores GC 19 and GC 22 exhibit values that ranges from 0.2‰ and 0.8‰ to -0.6‰ and -0.4‰, respectively (tables 4 and 6, figures 16 and 18).

4.3.2.1 $\delta^{18}O$ isotope values:

The foraminiferal $\delta^{18}O$ data of the four studied cores shows similar patterns. For example, the very upper sediments of the core, which are the one deposited more recently, has a low isotope $\delta^{18}O$ values of below 3‰ (tables 3-5, figures 15-17). The exception being core GC 22, in which the foraminiferal $\delta^{18}O$ values are almost 3.5‰ (table 6, figure 18). On the other hand, the lower half of the cores containing the oldest sediments have higher values of $\delta^{18}O$, between 4‰ and 5‰ (tables 3-6, figures 15-18). In three of the four cores (GC 3, GC 19, GC 20), there is also one distinct low in $\delta^{18}O$, value of the most recent sediments (around 3‰).

5 Discussion:

The results of this study demonstrate that methane seepage occurred during the Pleistocene at Vestnesa Ridge. In particular, cores GC 3 and GC 20 magnetic susceptibility and planktic foraminiferal $\delta^{13}C$ records show past methane emissions at these sites. No signs of past methane seepage were detected in cores GC 19 and GC 22. In order to place these findings in a temporal context, detailed stratigraphic correlations were done using magnetic susceptibility measurements, core lithologies, and planktic foraminiferal $\delta^{18}O$ values. Because cores GC 3 and GC 20 original magnetic susceptibility signals were low, which is typical at methane seeps, for these cores MS could not be used for correlation purposes.

In the context of other published studies, the results of this thesis contribute to the understanding of past and present methane emissions in the Vestnesa Ridge area and Western Svalbard.

5.1 Chronology and core correlations

The results of the studied cores from Vestnesa Ridge were compared to results obtained from cores from the western Svalbard slope published by Jessen et al. (2010) in order to place the investigated core in a chronostratigraphic framework and provide ages for distinct sedimentary units.

5.1.1 Magnetic susceptibility:

The magnetic susceptibility from the four cores that was studied were all done by the same instrument at The Arctic University of Norway, in Tromsø. The results obtained were compared with the magnetic susceptibility record from Jessen et al. (2010). This record was made by stacking the magnetic susceptibility (MS) graphs made from the different cores, then these graphs were normalized because the MS on the different cores was measured using different instruments. This was not necessary for the cores analysed in this study, as the MS was analysed in the same laboratory following the same procedure Then, AMS^{14}C data and the oxygen isotope records were used to make sure that the stacked record of the MS was correct (Jessen et al., 2010). After stacking, the ^{14}C and calibrated ages were used to generate a common age model for all cores based on linear best fit. This stacked record was used to correlate the records of the cores analysed in this study (GC 3, GC 19, GC 20, GC 22). As this stacked record also contains some AMS^{14}C ages, it can be used as a reference to provide ages

for the lithological changes and sedimentary units identified in the studied cores (i.e., the diatom-rich layer, laminated layer and mass transported layer). A complete sedimentary record including MS measurements and ages for the Western Svalbard slope during the Last Glacial Maximum (LGM), the deglaciation and Holocene are found in core JM03-373PC2 presented in Jessen et al. (2010). In Jessen et al. (2010) are the two low intervals dated, the oldest interval is dated >22,450cal years BP while the youngest dates between 15,160 and 14,380cal years BP. Between the two low marked intervals is an interval with higher and more variated MS measurements. The interval with variated MS values is clearly observed in core GC 19 (figure 11). This interval is from the lower deglaciation and the Last Glacial Maximum (LGM). Higher up in the GC 19 core is an section of increasing MS measurements, this is corresponding with MS values from Jessen et al. (2010) and has been dated to 9920 to 8170cal years BP. After 8170cal years BP does the MS measurements gradually decreases towards the top of the core and the most recent sediments. Both the section with increasing MS values and the section with decreasing MS values are from the Holocene period.

5.2 Lithology

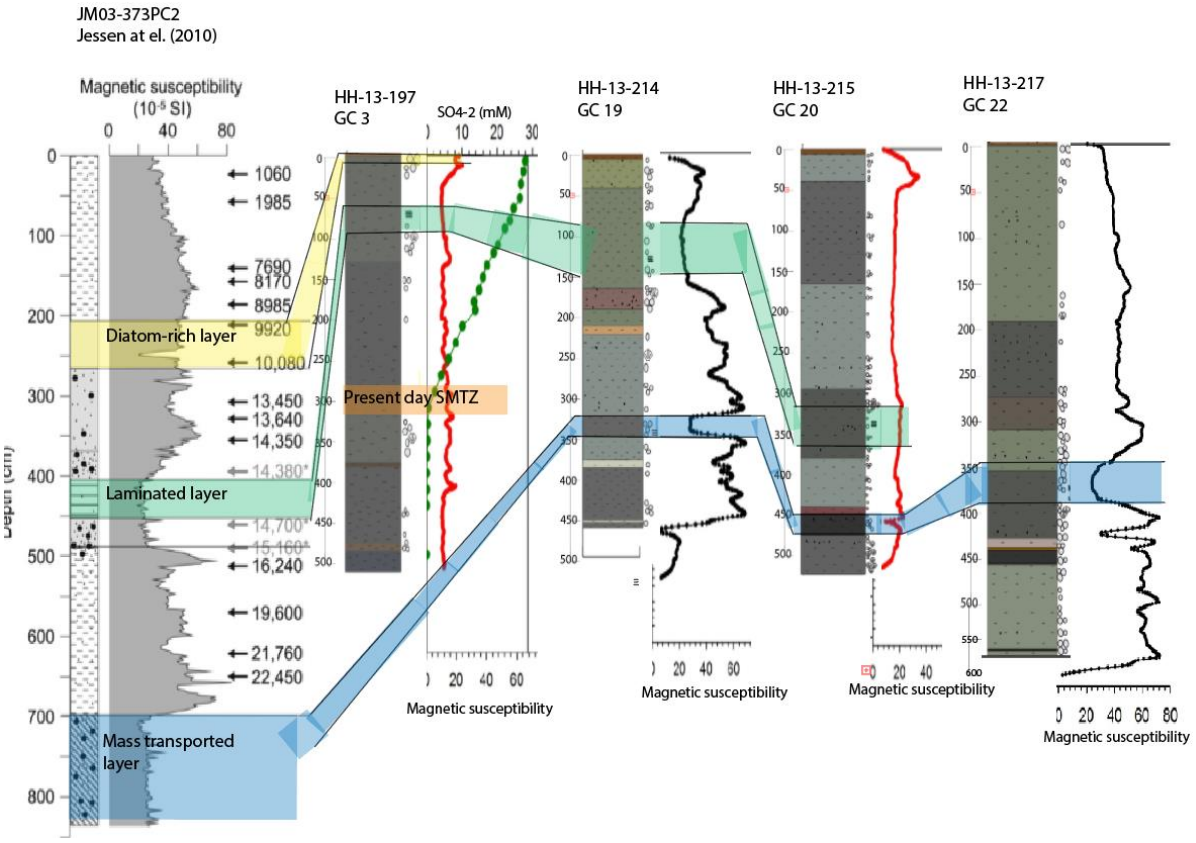

Figure 19 –Lithology, MS graphs and dates form Jessen at el. (2010) compared to lithology and MS graphs from the studied cores.

There are some distinct sedimentary units recognized in the four studied cores: a diatom-rich layer, a laminated layer and a very dark unsorted mass transport deposit thick layer (figure 19). These different distinct units are also discussed in the article written by Jessen et al. (2010). Jessen et al. (2010) is therefore used to compare the observations of these layers and correlate them with the core JM03-373PC2 which contains tie points and AMS^{14}C dates.

5.1.2 Mass transport deposits:

Three of the four studied cores (GC 19, GC 20, GC 22) have a very dark coarse unsorted layer, with the exception of core GC 3 (figure 19). This unsorted layer contains a lot of sharp pebbles and cobbles in a clayeysilty matrix. The magnetic susceptibility is low. In the three cores where this layer was found, its thickness varied from about 20cm to about 50cm.. The unsorted mass transport deposit is dated from 24,080 ± 150 to 23,550 ± 185cal years BP (Jessen et al., 2010). In Jessen et al. (2010), some of the mass transport deposits were interpreted as debris flow deposition, whereas in one core it was interpreted as a possible turbidite. For the possible turbidite, the deposit is characterized by clay matrix with dark colour laminations. Core GC 20 and GC 22 has similar deposits: unstructured, with abundant sharp centimetric pebbles and cobbles in a clay matrix and core GC 19 also exhibits dark colour laminations.

Interpretation:

This very dark grey coarse unsorted layer which is found in three of the studied cores (GC 19, GC 20, GC 22) is the same sedimentary unit found in several cores by Jessen et al. (2010). It is a unit which was deposited by mass transport processes. Core GC 20 and GC 22 were possibly deposited by debris flow as they are structureless and contains a lot of pebbles and cobbles in a clay matrix. While core GC 19 has laminations and a dark colour within the unsorted layer, which suggest a possible turbidite.

The mass transport deposits was dated by using the hemipelagic sediments overlaying the unsorted layer. These sediments were dated by AMS^{14}C and gave a minimum age of the various mass transport deposits that occurred along the Western Svalbard margin. Besides these AMS^{14}C ages, the age of the turbidite layer and of a debris flow are used for stratigraphic purposes. This turbidite has an minimum age of 23,050 ± 210cal years BP and an maximum age of 25,370 ± 235cal years BP (Jessen et al., 2010).The debris flow maximum age was 23,440 ± 315cal years BP. Using all these ages, it was possible to constrain the mass transport deposits upper and lower ages, which was used to date the studied cores.

5.1.3 Laminated sediments:

Fine-grained laminated sediment layers are found in three of the studied cores (GC 3, GC 19, GC 20). The lamination is seen in an olive to grey coloured very fine-grained clay with few pebbles. It has a low magnetic susceptibility and it is found right above a clast rich clay layer. A similar laminated layer was found in cores studied by Jessen et al. (2010), and it was dated between 14,700 ± 225 and 14,380 ± 220cal years BP.

Interpretation:

The laminated layer was deposited during the early Bølling interstadial. This indicated that the event or events occurred around 14,400cal years BP, and that it lasted for less than 3-4 centuries. These laminated sediments are interpreted as a result of a rapid sedimentation that originated from turbid meltwater that occurred as the Svalbard-Barents Sea Ice Sheet retreated. There is a possibility that the widespread layers may be the result of one large meltwater outburst event, that happened near synchronous (Jessen et al., 2010). This event is observed in three of the studied cores (GC 3, GC 19, GC 20). The magnetic susceptibility of the laminated sedimentary unit is low and increases below the lower boundary of the laminated layer.

5.1.4 Diatom-rich layer:

Core GC 3 is characterized by a very fine-grained and structureless layer. This layer contained diatoms. In the cores examined by Jessen et al. (2010), this layer was found to be between 35-65cm thick, whereas in core GC 3 this layer was located at 5cm and it was 10cm thick. The diatom rich layer consist of a hemipelagic very fine grained mud that originated from the early Holocene between 10,100 ± 150 and 9840 ± 200cal years (Jessen et al., 2010).

Interpretation:

The diatom layer represents an early Holocene diatom maximum and can be linked to the northward movement of the Polar front (Jessen et al., 2010). This diatom maximum is found both in the Fram Strait and in the southern Norwegian Sea. Because it was found that the diatom-rich layer has a consistent age, with a dating error of ± 200cal years, on the Svalbard slope, this layer can be used as a chronostratigraphic marker in cores collected from this area. The upper and lower boundary for this layer can be used to set a date for the diatom rich layer found in core GC 3.

5.2 Foraminifera:

In this study, the planktic foraminiferal $\delta^{13}C$ values were used to investigate past episodes of methane seepage at the sampling sites. Instead, the planktic foraminiferal $\delta^{8}O$ values were used for stratigraphic purposes.

5.2.1 $\delta^{13}C$ isotope analyses:

Two of the studied cores, core GC 19 and GC 22 exhibit $\delta^{13}C$ of *N. pachyderma* in the range between 0 and -0.6‰ and can be considered as representative of normal marine conditions (Knies and Stein, 1998). The slightly negative values are probably the $\delta^{13}C$ values of the Barents Sea and the waters around Svalbard at the period when the foraminifera was growing and therefore recording the chemical components of the oceanwater surrounding them (Armstrong & Braiser, 2013). The $\delta^{13}C$ values of foraminifera are for most controlled by global shifts that occurs during changes in terrestrial vegetation and /or when sedimentary organic matter oxides as a result of a large-scale burial. These values are also influenced by export production, deep-water age and respiration at depth (Panieri, et al., 2016). There is a peak for the $\delta^{13}C$ values of around -0.5‰ in core GC 19 and GC 22 that seems to be recorded during the LGM, as the $\delta^{13}C$ values decline during periods with colder glacial oceans due to greater oxidation of organic matter (Armstrong & Braiser, 2013). The more distinctly negative $\delta^{13}C$ values of core GC 3 and GC 20, -15‰ and -12‰, respectively indicates past seepage of methane from the area. Both of the cores were taken from pockmarks at Vestnesa Ridge.

The negative isotope values of -10‰ and -15‰ from the foraminifera tests within two of the studied cores (GC 3, GC 20) indicate the presence of methane-derived authigenic carbonate (MDAC) that precipitated around the foraminifera test at the sulphate methane transition zone (SMTZ). Thus, the foraminiferal original isotopic composition have been influenced by diagenetic alterations that occurred at SMTZ after the death and burial of the organism (Panieri, al., 2016; Schneider et al., 2018). The MDAC precipitation at SMTZ adds a second phase of carbonate that is depleted in $\delta^{13}C$ on the foraminifera tests. Because of this, diagenetically altered foraminifera show negative $\delta^{13}C$ values. The negative $\delta^{13}C$ values found in Schneider article has a range of -7 to -36‰ (Schneider et al., 2018). In the article by Panieri et al. (2016) negative $\delta^{13}C$ values from the foraminifera tests ranged from -5 to -15‰. Also in this case, the signal was interpreted as being caused by the presence of secondary overgrowth deposited at the SMTZ as a consequence of enhanced methane flux. The SEM EDS investigations of foraminifera that exhibit depleted $\delta^{13}C$ values revealed high-Mg calcite

crystals on the exterior and internal walls of the tests (Schneider et al., 2017). For foraminifera tests with clear evidence of secondary overgrowth, the high-Mg calcite crystal created a solid crust on the exterior and interior walls. For the cores influenced by methane emission in the past (GC 3 and GC 20) the studied foraminifera tests show poorer conditions and tests covered by high-Mg crystals (table 3 and 5).

Diagenetically altered foraminifera and stable isotopes have been explored to establish where and when the methane venting occurred during the last deglaciation. Panieri et al. (2016) showed $\delta^{13}C$ values from foraminifera were collected from cores taken close to active methane seepage offshore Western Svalbard, at the present day GHSZ limit (around 400m) or at shallower water depths that would have been within the GHSZ limit in the past. Foraminiferal $\delta^{13}C$ values ranged from -1.68‰ to -11.44‰. Together with these low values there are some very old radiocarbon dates (uncorrected AMS^{14}C ages that range from 40,3 to > 52ka) which is found in cores from the GHSZ limit. These two combined implies that methane is the dominant source of carbon when it comes to the carbonate overgrowth that has precipitated on the foraminifera tests. The incorrect very old radiocarbon AMS ^{14}C dates and the negative $\delta^{13}C$ values comes as an result of some fossil ^{14}C-free methane that has been incorporated into the carbonate precipitated around foraminiferal tests. The negative $\delta^{13}C$ values from the foraminifera tests may be caused by either oxidation of organic matter or methane that has been oxidized to CO_2 by methanotrophic archaea. In the article by Panieri et al. (2016) they conclude that the second option is more likely than the first, as the area where the cores are taken from is near the GHSZ limit and the site has an abundance of methane flares. After studying the foraminifera tests with scanning electron microscopy (SEM),it was observed that the foraminifera test from cores within the GHSZ limit with normal $\delta^{13}C$ values were pristine, while the foraminifera tests from the cores with negative $\delta^{13}C$ values have both internal and external overgrowth of secondary calcite, this was observed in the article by Panieri et al. (2016). Similar observation were found in the cores studied in this master project.

5.2.2 $\delta^{18}O$ isotope analyses:

The data obtained are consistent with the $\delta^{18}O$ stratigraphy for planktic foraminifera from the north-western Svalbard margin during the Last Glacial Maximum (LGM), the deglaciation and Early Holocene. This gives the possibility to provide an important chronological framework for stratigraphic correlation. In Panieri at el. (2016) there is a decrease in $\delta^{18}O$ values from the foraminifera tests at the beginning of the Holocene at about 10,000 years BP,

where the $\delta^{18}O$ values declined from around 4‰ to 2‰. Around 15,000 years BP there were spikes in $\delta^{18}O$ values towards the range found during Holocene age, these spikes was caused by a local meltwater event 1A and continued to about 20,000 years BP. Which fits good with the $\delta^{18}O$ lows in the studied cores, especially core GC 19 and core GC 20. There was an continue supply of terrigenous sediments at about 14,600 years BP that occurred simultaneously and cause a ~20m rise in sea level. The rise in sea level happened in less than 500 years during the Bølling-Allerød interstadial. The low $\delta^{18}C$ values from foraminifera tests that is from the end of the melt water event A1 during Bølling-Allerød is represented in my cores by the laminated sediments dated to 14,700 to 14,380cal years BP by Jessen et al. (2010). During the LGM the $\delta^{18}O$ values were within a range from 4.5‰ to 4.8‰. Similar results are found in all the studied cores. During meltwater event A1 found in post LGM sediments there was a decrease in $\delta^{18}O$ values in the range from 2.8‰ to 3‰. During the Younger Dryas the less distinct negative $\delta^{18}O$ value, were caused by northward protruding warm Atlantic water masses which lead to a destabilisation of tidewater glaciers resulting in local meltwater pulses in the northern North Atlantic. This signalled the beginning of interglacial conditions.

6 Conclusion:

- It was established a stratigraphic framework for the investigated sediment cores collected on the crest of the Vestnesa Ridge at 1200m water depth using the existing stratigraphic marker horizons defined for the western Svalbard margin according to Jessen et al. (2010). The defined stratigraphic marker horizons which have been described here as sedimentary units and used to correlate the cores are: a very dark grey layer rich in clast/pebbles with laminated sediments which exhibit a very low MS profile (within the LGM; between 24,080 ± 150 to 23,550 ± 185cal years BP), a fine-grained laminated sediments (Bølling interstadial; between 14,700 ± 225 and 14,380 ± 220cal years BP), and a diatom-rich layer (rich in *Coscinodiscus spp*. Diatoms) (Early Holocene; between 10,100 ± 150 and 9840 ± 200cal years).

- The state of preservation of foraminifera is diverse among samples and within the same sample, with some tests in pretty good conditions and others in a poorer

conditions. There are some indications of methane seepages at cores GC 3 and GC 20, which have a poorer preservation of foraminifera than core GC 19 and GC 22. Some of the foraminiferal tests that were observed under the microscope had grey crystals on them, and show a bad state of preservation. These grey crystals originated during precipitation of MDAC which can occur as secondary overgrowth on foraminiferal tests. This secondary overgrowth, which causes low $\delta^{13}C$ values, is an indicator of sediments and foraminifera affected by methane seepage. The secondary overgrowth precipitates at SMTZ and since this biochemical horizon does not follow the sedimentation of the studied cores it is not possible to date the methane emission events because the precipitation time of the secondary overgrowth does not necessarily coincide with the age of the host sediments. The studied cores which were affected by methane seepage were collected from the crest of the southern portion of Vestnesa Ridge (active seepage area), from sites within pockmarks with no flares and from inactive pockmarks with no flares. The permeable sediments allow methane to rise upwards. Faults also contributes to methane seepage and some faults were identified in the area. The GHSZ is a moveable zone which moves higher in the sediment column during cold periods while during warmer periods, the GHSZ becomes deeper and the more superficial hydrates start dissociating fuelling a higher methane flux and a shallower SMTZ. These conditions are meet in two of the studied cores (GC 3 and GC 20). The planktic foraminiferal $\delta^{13}C$ values measured in cores GC 19 and GC 22 represent normal $\delta^{13}C$ values. Thus, these cores were not affected by methane seepage. Core GC 22 was the core taken outside the area of observed flares and seepage activity (reference core). However, core GC 19 was collected at a location with flares indicating an active seepage area. Even so, core GC 19 magnetic susceptibility and planktic foraminiferal $\delta^{13}C$ values were not influenced by methane. These results suggest that the location where core GC 19 was collected only recently became an active site. This is not surprising because seepage sites are very dynamic and methane can move from site to site (few centimetres or meters away).

- The $\delta^{18}O$ isotope results are affected by the same events as discussed in Jessen et al. (2010) and Schneider et al. (2018), with the lower values related to spikes in melt water events during the deglaciation (around 15,000 to 20,000 years BP). This is likely for at least cores GC 19 and GC 20, where the depth of the low $\delta^{18}O$ values is in-between the laminated sediments deposited during Bølling-Allerød interstadial and

the mass transported sediments deposited during the LGM. In core GC 3, low $\delta^{18}O$ values were measured near the top, right below the laminated layer dated by Jessen et al. (2010) to about 14,380 to 15,160 years BP. In core GC 22, the $\delta^{18}O$ values below about 175cm depth can be considered relatively higher isotope values, most likely indicating colder periods, as the $\delta^{18}O$ increases during times of glacial conditions (Armstrong & Braiser, 2013).

7 Attachments:

Foraminifera study tables for all studied cores, with sample depth, number of picked foraminifera, description of the foraminifera state of preservation, observations of the sediments, and isotopic measurements ($\delta^{18}O$ and $\delta^{13}C$).

			Foraminifera (counting and color)						Isotop analysis (marked sample		Isotop anaysis result (of marked samples)	
Core HH-197 GC 3			Benthic		Planktic	Forams	Grains (> 100µm)		C. neoteretis	N. pachyderma	C. neoteretis	N. pachyderma
samples dept	sectio	marked as	Cassidulina neoteretis		Neogloboquedrina pachyder	Describtion	Describtion					d13C VPDB [‰]	d18O VPSB [‰]
0-1cm	1	197/1/0-1cm	21	white	23	white	Not so many forams, good condition	Many bigger and smaller grains, light (brown) in color	1	1		-0,25	2,70
10-11cm	1	197/1/10-11cm	21	white	24	white, grey/yellow	Some forams, but not many. Good condition	Lots of small grains, light in color	2	2		-0,01	2,87
20-21cm	1	197/1/20-21cm	21	white, transpherent	21	white, grey/yellow	Not that many forams, good condition	Much small grains, light in color	3	3		-0,23	4,04
30-31cm	1	197/1/30-31cm	21	white	21	white, grey/yellow	Few forams, espesially planktic, good condition	Long shimmery brown material. Small ligth colored grains.	4	4		-0,52	4,05
40-41cm	1	197/1/40-41cm	2	white	21	white, grey/yellow	Few forams, espesially benthic, good condition	Long shimmery brown material. Bigger angular grains, cemented					
50-51cm	1	197/1/50-51cm	7	white	4	white	Very few forams, some broken.	Long shimmery brown material. Small ligth colored grains.					
60-61cm	1	197/1/60-61cm	21	white	11	white	Few forams, some broken.	Long shimmery brown material. Small ligth colored grains.	5	5		-0,88	3,78
70-71cm	1	197/1/70-71cm	13	white	26	white	Few benthic, many planktic forams. Some broken.	Small, light colored grains	6	6		-1,59	4,44
80-81cm	1	197/1/80-81cm	8	white	9	white	Few forams, some broken.	Much small grains, light in color					
90-91cm	1	197/1/90-91cm	23	white	1	a bit grey	Many benthic, 1 planktic forams. Good condition	Small, light colored grains. Some long brown material.	7				
100-101cm	2	197/2/0-1cm	36	white	0		Only benthic forams, good condition	Small brown/grey grains, a few transpherent. Very few bigg	8				
110-111cm	2	197/2/10-11cm	25	white	25	white, grey/yellow	Many benthic, few planktic forams. Many broken.	Much small, light colored grains.	9	7		-8,72	4,28
120-121cm	2	197/2/20-21cm	22	white	21	white, grey/yellow	Many benthic, very few planktic. Good condition	Much small, light colored grains. Some bigger grains too.	10	8		-3,93	4,25
130-131cm	2	197/2/30-31cm	20	white	24	white, grey/yellow	Many forams. Good condition.	Much small, light colored grains. Some bigger grains too.	11	9		-2,18	3,73
140-141cm	2	197/2/40-41cm	20	white	27	white, grey/yellow	Many forams. Good condition.	Mainly small, light colored grains.	12	10		-1,21	2,77
150-151cm	2	197/2/50-51cm	26	white	26	white, grey/yellow	Many forams. Good condition.	A lot of transpherent, light colored, small grains.	13	11		-1,01	3,58
160-161cm	2	197/2/60-61cm	22	white	20	white, grey/yellow	Many forams. Good condition.	A lot of transpherent, light colored, small grains.	14	12		-1,38	4,69
170-171cm	2	197/2/70-71cm	29	transpherent, white	45	white, grey/yellow	A lot of forams, espesially planktic. Good conditic	Much small, light colored grains.	15	13		-0,63	4,56
180-181cm	2	197/2/80-81cm	21	transpherent	38	white, grey/yellow	A lot of forams, espesially planktic. Good conditic	Much small, light colored grains.	16	14		-0,81	4,76
190-191cm	2	197/2/90-91cm	36	white	44	white, grey/yellow	Many forams, espesially planktic. Good condition	Much small, light colored grains.	17	15		-1,72	4,71
200-201cm	3	197/3/0-1cm	21	white	35	white, grey/yellow	Many forams, espesially planktic. Good condition	Small, light colored grains	18	16		-1,33	4,67
210-211cm	3	197/3/10-11cm	20	white	36	white, grey/yellow	Many forams, espesially planktic. Good condition	Small, light colored grains	19	17		-1,26	4,73
220-221cm	3	197/3/20-21cm	16	white	70	white, grey/yellow	Many planktic forams, few benthic. Some broken	Most transpherent grains, some bigger grains. Elongated	20	18		-0,83	4,68
230-231cm	3	197/3/30-31cm	22	white	34	white, grey/yellow	Many forams, espesially planktic. Good condition	Small, light colored grains	21	19		-0,62	4,61
240-241cm	3	197/3/40-41cm	20	white, golden	32	white, grey/yellow	Many forams, espesially planktic. Good condition	Small, light colored grains	22	20		-1,46	4,66
250-251cm	3	197/3/50-51cm	28	transpherent	22	white, grey/yellow	Many forams, espesially planktic. Good condition	Few grains, mainly light colored, small grains.	23	21		-0,64	4,62
260-261cm	3	197/3/60-61cm	30	white	22	white, grey/yellow	Many forams. Good condition	Few grains, mainly light colored, small grains.	24	22		-1,01	4,77
270-271cm	3	197/3/70-71cm	23	transpherent	40	white, grey/yellow	Very many planktic, few benthic forams. Good con	Very few grains. Mainly light colored, small grains	25	23		-0,69	4,79
280-281cm	3	197/3/80-81cm	22	transpherent	42	white, grey/yellow	Many forams, espesially planktic. Good condition	Few grains, mainly light colored, small grains.	26	24		-0,54	4,77
290-291cm	3	197/3/90-91cm	23	transpherent	26	white, grey/yellow	Very many planktic, few benthic forams. Good con	Few grains, mainly light colored, small grains.	27	25		-0,60	4,71
300-301cm	4	197/4/0-1cm	27	white, transpherent	32	white	A lot of planktic, fewer benthic forams. Good con.	Small, light colored, many transpherent grains.	28	26		-0,69	4,75
310-311cm	4	197/4/10-11cm	28	white, transpherent	25	white, grey/yellow	Many benthic, fewer planktic forams. Good con.	Few grains, mainly light colored and small.	29	27		-0,92	4,69
320-321cm	4	197/4/20-21cm	25	white, transpherent	28	white, grey/yellow	Many planktic, fewer benthic forams. Good con.	Many grains, mainly small, light colored grains.	30	28		-1,00	4,73
330-331cm	4	197/4/30-31cm	24	white, transpherent	26	white, grey/yellow	Very few forams, lots of broken ones.	Very much grains. Mainly small, light colored grains.		29		-5,39	4,74
340-341cm	4	197/4/40-41cm	20	white, transpherent	21	white, grey/yellow	Very few forams. Not a good condition	Much grains, mainly small, light colored grains.	31	30		-1,33	4,31
350-351cm	4	197/4/50-51cm	12	white, transpherent	7	white, grey/yellow	Few forams. Not a good condition	Small and light colored grains. Some bigger grains too.					
360-361cm	4	197/4/60-61cm	29	white, transpherent	18	white, grey/yellow	Few forams, epesially planktic. Not a good con.	Much grains, mainly grey in color, but also transpherent. S	32	31		-4,94	4,66
370-371cm	4	197/4/70-71cm	9	white, transpherent	2	white, grey/yellow	Few forams. Not a good condition	More bigger grains, darker in color. Some big transpherent ones.					
380-381cm	4	197/4/80-81cm	23	white, transpherent	24	white, grey/yellow	Lots of forams. Ok condition.	Fewer grains, mainly small, light colored grains.	33	32		-0,71	4,61
390-391cm	4	197/4/90-91cm	24	white, transpherent	25	white, grey/yellow	Very many forams. Ok condition. (dark spots)	Few grains, mainly light colored and small.	34	33		-1,03	4,51
400-401cm	4	197/4/100-110cm	21	white, transpherent	27	white, grey/yellow	Many planktic, fewer benthic forams. Good con.	Small, light colored grains.	35	34		-0,43	4,44
									36			-0,25	4,24
408-409cm	5	197/5/8-9cm	21	white	40	white, grey/yellow	Nearly only planktic forams. Ok condition	Few grains, mainly small, light colored ones.	37	37		-0,33	4,24
418-419cm	5	197/5/18-19cm	22	white	30	white, grey/yellow	Not many forams, many broken ones. Not good c	Many small, light colored grains.	38	38		-0,46	4,24
428-429cm	5	197/5/28-29cm	29	white, golden	24	white, grey/yellow	Many forams, good condition.	Small, light colored grains.	39	39		-0,72	4,24
438-339cm	5	197/5/38-39cm	32	white	31	white, grey/yellow	A lot of forams, espesially planktic. Good con.	Small, light colored grains.	40	40		-1,06	4,24
448-449cm	5	197/5/48-49cm	24	white	28	white, grey/yellow	A lot of forams, espesially planktic. Good con.	Small, light colored grains.	41	41		-3,66	4,24
458-459cm	5	197/5/58-59cm	23	white	28	white, grey/yellow	A lot of forams, good con.	Small, light colored grains.	42	42		-2,36	4,24
468-469cm	5	197/5/68-69cm	25	white	20	white, grey/yellow	Fewer forams, espesially benthic.	Small, light colored grains.	43	43		-3,28	4,24
478-479cm	5	197/5/78-79cm	2	white	16	white, grey/yellow	Very few forams, espesially benthic. ok condition.	Small, light colored grains.		44		-0,44	4,24
488-489cm	5	197/5/88-89cm	40	white	21	white, grey/yellow	Many forams, espesially benthic. Some broken	Much small transpherent grains, some light colored grains	44	45		-5,30	4,24
498-499cm	5	197/5/98-99cm	2	white	18	white	Few forams, espesially benthic. Good condtion	Much silvery, small grains. Also a lot of transpherent ones.		46		-4,07	4,24
505-506cm	5	197/5/105-106cm	14	white	28	white, grey/yellow	Few forams, espesially benthic. Good condtion	Much transperent, small grains.	45	47		-1,35	4,24
514-515cm	5	197/5/114-115cm	8	white	20	white, grey/yellow	Few forams, espesially benthic. ok condtion	white shinny spots on grains. Some transpherent grains.		48		-0,11	4,24
423-424cm	5	197/5/423-424cm	3	white	11	grey, yellow, white	Bad condition, lots of brownish spot	extra sample	Much small grey/browish grains. Some elongated grey cemented materia	49			
446-447cm	5	197/5/446-447cm	25	transpherent	26	white, yellow/grey	Moderate condition.	extra sample	Much small grey/browish grains. Some bigger grey grains.	46	50	-1,48	4,24

Core HH-13-214 GC 19			Foraminifera (counting and color)		Forams describtion			Isotop analysis (marked samp		Isotop anaysis result (of marked samples)		
										Benthic	Planktic	
			Benthic	Planktic	Benthic	Planktic	Grains (>100µm)	Benthic	Planktic	C. neoteretis	N.pachyderma	
sample depth (cr	section	marked as (cr	Cassidulina neoteret	Neogloboquedrina pachyderma	Cassidulina neoteretis	Neogloboquedrina pachyderma	Describtion	C.neoteretis	N. pachyderma		d13C VPDB [‰]	d18O VPSB [‰]
1-2	1	214/1/1-2	22 transpherent/whit	25 white	few forams, some structur and shine, better-moderate condition	few forams, moderate condition some holes	Small ligth grains, lots of transpherent treads	47	51		0,15	2,92
11-12		214/1/11-12	21 transpherent/white	24 white	few forams, some structur and shine, better-moderate condition	moderate condition some holes	Small ligth grains, lots of transpherent treads	48	52		0,13	3,26
21-22		214/1/21-22	14 white/transpherent	14 white	few forams small sample, little structur and shine, moderate condition	small sample, moderate-better condition	Lots of small transpherent shinny grains	49	53		-0,03	3,31
31-32		214/1/31-32	21 white/transpherent	22 white	many forams small sample, some structure and shine, better condition	small sample, moderate-better condition	small transpherent grains, some cemented grains	50	54		-0,43	4,03
41-42		214/1/41-42	26 white/transpheren	24 white	many forams, some structure and shine, better-moderate condition	moderate condition some holes	small cemented grains	51	55		-0,17	4,17
51-52		214/1/51-52	22 white/transpheren	22 white	many forams, some structure and shine, better-moderate condition	moderate condition some holes	lots of small brownish grain	52	56		-0,18	4,09
61-62		214/1/61-62	31 white/transpherent	27 yellow/white	many forams, little structure and shine, moderate condition	many forams, moderate condition some holes	small grey/brownish grains	53	57		-0,03	4,09
71-72		214/1/71-72	29 white/transpheren	18 yellow/white	many forams small sample, some structure and shine, moderate condition	small sample, moderate condition	small grey/brownish grains and some transpherent grains	54	58		-0,31	4,32
81-82		214/1/81-82	25 white/transpheren	30 yellow/white	small sample, some structure and shine, moderate condition	small sample many forams, moderate condition	small grey/brownish grains	55	59		-0,44	4,09
91-92		214/1/91-92	27 white/transpheren	27 white	very small sample many forams, little structure and shine, moderate conditior	very small sample many forams, moderate condition	Lots of small grey/brownish grains	56	60		-0,39	4,21
101-102	2	214/2/1-2	24 white/transpheren	27 white	very small sample many forams, some structure and shine, moderate conditi	very small sample many forams, moderate condition	Lots of small grey/brownish grains	57	61		-0,27	4,20
111-112		214/2/11-12	27 white	4 white	very small sample many forams, little structure and shine, moderate conditior	very small sample few forams, moderate condition	Lots of small grey/brownish grains	58				
121-122		214/2/21-22	30 white	35 white	very small sample many forams, little structure and shine, moderate conditior	very small sample many forams, better-moderate co	Lots of small grey/brownish grains, some transpherent treads	59	62		-0,53	4,14
131-132		214/2/31-32	35 white	4 white	many forams, little structure and shine, moderate condition	few forams, moderate condition	small brown/grey grains	60				
141-142		214/2/41-42	35 white/transpheren	27 white	many forams small sample, some structure and shine, moderate condition	many forams, moderate condition	small brown/grey grains	61	63		-0,23	4,40
151-152		214/2/51-52	23 white	27 white	small sample, little structure and shine, moderate condition	moderate-better condition	Lots of small grey/brownish grains	62	64		-0,56	4,16
161-162		214/2/61-62	25 white/transpheren	24 white	many forams, some structure and shine, better-moderate condition	moderate condition some holes	Lots of small grey/brownish grains	63	65		-0,13	4,43
171-172		214/2/71-72	30 white/transpheren	22 white	many forams, some structure and shine, better-moderate condition	moderate condition some holes	Lots of small grey/brownish grains, some cemented	64	66		-0,27	4,18
181-182		214/2/81-82	22 white/transpheren	28 white	few forams, little structur and shine, moderate condition	moderate condition some holes	Lots of small transpherent grains and grey/brownish grains	65	67		-0,16	3,86
191-192		214/2/91-92	22 white/transpheren	22 grey/white	little structure and shine, moderate condition	many forams, bad condition many gray ones	small grey grains	66	68		-0,26	2,62
201-202	3	214/3/1-2	25 white/transpheren	28 white	some structure and shine, moderate-better condition	many forams, moderate-better condition	small grey grains	67	69		-0,10	4,75
211-212		214/3/11-12	22 white/transpheren	25 white	some structure and shine, moderate-better condition	many forams, moderate-better condition	small grey grains	68	70		-0,33	3,41
221-222		214/3/21-22	27 white/transpheren	24 white	many forams, some structure and shine, better condition	many forams, moderate-better condition	small grey grains	69	71		-0,02	4,90
231-232		214/3/31-32	23 white/transpheren	26 white	some structure and shine, moderate-better condition	many forams, moderate condition	small grey grains	70	72		0,00	4,68
241-242		214/3/41-42	30 white/transpheren	24 white/grey	many forams, some structure and shine, moderate-better condition	many forams, moderate condition	small grey grains	71	73		0,00	4,83
251-252		214/3/51-52	23 white/transpheren	29 white	many forams, some structure and shine, moderate-better condition	many forams, moderate-better condition	small grey grains	72	74		-0,27	4,55
261-262		214/3/61-62	24 white/transpheren	24 white	many forams, some structure and shine, moderate-better condition	many forams, moderate-better condition	small grey grains	73	75		0,04	4,88
271-272		214/3/71-72	35 white/transpheren	25 white	many forams, some structure and shine, moderate-better condition	many forams, moderate-better condition	small grey grains, some black treads	74	76		-0,22	4,64
281-282		214/3/81-82	24 white/transpherer	26 white	many forams, some structure and shine, moderate-better condition	many forams, moderate-better condition	small grey grains	75	77		-0,05	4,67
291-292		214/3/91-92	23 white/transpherer	26 white	many forams, some structure and shine, moderate-better condition	many forams, moderate-better condition	small grey grains	76	78		0,09	4,84
301-302	4	214/4/1-2	21 white/transpheren	25 white/grey	many forams, some structure and shine, moderate-better condition	many forams, moderate condition	small grey grains	78	80		-0,05	4,58
311-312		214/4/11-12	24 white/transpheren	23 white/grey	many forams, some structure and shine, moderate condition	many forams, moderate condition	small grey grains	79	81		-0,03	4,76
321-322		214/4/21-22	1 white	8 white	very few forams big sample, little structure and shine, moderate condition	few forams big sample, moderate condition	lots of bigger grains					
331-332		214/4/31-32	4 transpherent	2 white	very few forams big sample, some structure and shine, moderate condition	very few forams big sample, moderate condition	lots of bigger grains					
341-342		214/4/41-42	0	25 white		moderate condition	small grey grains		82		-0,10	4,71
351-352		214/4/51-52	24 white/transpheren	27 white	many forams, some structure and shine, moderate-better condition	many forams, moderate condition	small grey grains	80	83		-0,11	4,46
361-362		214/4/61-62	23 white/transpheren	30 white	many forams small sample, some structure and shine, moderate-better cond	many forams small sample, moderate condition	small grey grains	81	84		-0,08	4,11
371-372		214/4/71-72	18 white/transpherent	24 white	many forams very small sample, little structure and shine, moderate-better co	many forams very small sample, moderate condition	small grey grains	82	85		-0,09	4,52
381-382		214/4/81-82	0	17 white/grey		few forams, moderate condition	lots of transpherent grains		86		0,06	4,31
391-392		214/4/91-92	23 white/transpheren	23 white/grey	many forams small sample, some structure and shine, moderate-better cond	many forams small sample, moderate condition	small grey grains	83	87		-0,03	4,53
401-402	5	214/5/1-2	24 white/transpheren	24 white/grey	many forams, some structure and shine, moderate condition	many forams, moderate condition	small grey grains	85	89		-0,38	4,27
411-412		214/5/11-12	2 transpherent	25 white	very few forams, some structure and shine, moderate condition	many forams, moderate-better condition	small brownish cemented grains		90		0,08	4,28
421-422		214/5/21-22	23 white/transpheren	23 white/yellow	many forams, some structure and shine, moderate-better condition	many forams, moderate-better condition	small grey/brownish grains	86	91		-0,38	4,06
431-432		214/5/31-32	3 white/transpherent	23 white	very few forams, little structure and shine, moderate condition	moderate-better condition	small grey/brownish grains some cemented, some transpherent grains		92		0,04	4,43
441-442		214/5/41-42	24 white/transpheren	25 white	some structure and shine, moderate-better condition	moderate condition some holes	small cemented brownish grains	87	93		-0,12	4,38
451-452		214/5/51-52	30 transpherent	33 white/grey	many forams, some structure and shine, better condition	many forams, moderate condition	small grey/brownish grains	88	94		0,08	4,15
Extra samples												
207-208	3	214/3/07-08	22 white/transpheren	23 white/yellow	many forams, some structure and shinne, moderate condition	many forams, moderate condition	small grey grains	77	79		-0,31	4,62
388-389	4	214/4/88-89	32 white/transpheren	29 white/yellow/grey	many forams, some structure and shinne, moderate-better condition	many forams, moderate condition	much small grey grains	84	88		-0,20	4,54
447-448	5	214/5/47-48	17 white/transpherent	2 white	some structure and shinne, moderate condition	moderate condition	small cemented grey/brownish grains	89				

Core HH-13-215 GC 20			Foraminifera (counting and color)		Forams describtion			Isotop analyisis (marked samples)		Isotop anaøysis (of marked samples)			
										Benthic	Planktic		
			Benthic	Planktic	Benthic	Planktic	Grains (>100µm)	Benthic	Planktic	C. neoteretis	N. pachyderma		
sample depth (cr	section	marked as (cr	Cassidulina neoteretis	Neogloboquedrina pachyderma	Cassidulina neoteretis	Neogloboquedrina pachyderma	Describtion	C. neoteretis	N. pachyderma		d13C VPDB [‰	d18O VPDB [‰]	
1-2	1	215/1/1-2	25 transpherent/white	29 white	some structur and shine, moderate condition	moderate condition	Small grey/brownish grains, some cemented, lots of transpherent treads	90	95		0,23	2,95	
11-12		215/1/11-12	24 white	25 white/grey/yellow	some structur and shine, moderate condition	moderate condition	Small grey/brownish grains, some cemented, lots of transpherent treads	91	96		0,31	3,28	
21-22		215/1/21-22	25 white	30 white/grey/yellow	some structur and shine, moderate condition	moderate condition	Small grey/brownish grains, some cemented, lots of transpherent treads	92	97		0,33	2,99	
31-32		215/1/31-32	26 white/transpherent	37 white/grey/yellow	some structur and shine, moderate condition	moderate condition	Small grey/brownish grains, some cemented, lots of transpherent treads	93	98		0,48	3,33	
41-42		215/1/41-42	22 transpherent	28 white/grey/yellow	few forams small sample, some structur and shine, moderate-better condition	small sample, moderate condition	much small grey/brownish grains	94	99		0,57	3,63	
51-52		215/1/51-52	0	2 white	small sample	very few forams small sample, moderate condition	much small grey/brownish grains						
61-62		215/1/61-62	0	0	small sample	small sample	very much small grey/brownish grains						
71-72		215/1/71-72	0	0	small sample	small sample	very much small grey/brownish grains, some bigger transpherent grains						
81-82		215/1/81-82	2 white	27 white/yellow	very few forams, little structure and shine, moderate-bad condition	moderate condition	very much small grey/brownish grains, some bigger transpherent grains		100		0,17	4,28	
91-92		215/1/91-92	0	0	small sample	small sample	very much small grey/brownish grains, some bigger transpherent grains						
101-102	2	215/2/1-2	0	0	small sample	small sample	very much small grey/brownish grains, some bigger transpherent grains						
111-112		215/2/11-12	0	0	small sample	small sample	very much small grey/brownish grains, some bigger transpherent grains						
121-122		215/2/21-22	4 white	20 white	very few forams, little structure and shine, moderate-bad condition, some broken pieces	moderate condition some holes	much small grey/brownish grains, some cemented, transpherent treads, cylinder/grey organic material		101		0,16	3,55	
131-132		215/2/31-32	4 white	17 white	very few forams, little structure and shine, moderate-bad condition, some broken pieces	moderate condition some holes	much small grey/brownish grains, some cemented, transpherent treads, cylinder/grey organic material		102		0,33	3,55	
141-142		215/2/41-42	0	3 white	small sample	very few forams small sample, moderate-bad condition	much small grey/brownish grains, some cemented, transpherent treads, cylinder/grey organic material						
151-152		215/2/51-52	15 white	38 white/yellow/grey	few forams, little structur and shine, moderate condition	many forams, moderate-better condition	much small grey/brownish grains, a few cylinder/grey organic material	95	103		0,03	3,55	
161-162		215/2/61-62	26 white/transpherent	31 white	some structur and shine, moderate-better condition	many forams, moderate condition some broken ones	some small grey/brownish grains	96	104		0,03	3,55	
171-172		215/2/71-72	26 white/transpherent	26 white/yellow/grey	some structur and shine, moderate-better condition	many forams, moderate condition some broken ones	some small grey/brownish grains, some transpherent treads	97	105		0,03	3,55	
181-182		215/2/81-82	18 white/transpherent	25 white/grey/yellow	some structur and shine, moderate condition	many forams, moderate condition some broken ones	some small grey/brownish grains, some transpherent treads	98	106		0,03	3,55	
191-192		215/2/91-92	29 white	25 white/grey/yellow	some structur and shine, moderate condition	many forams, moderate condition some broken ones	some small grey/brownish grains, some transpherent treads	99	107		0,03	3,55	
201-202	3	215/3/1-2	23 white/transpherent	25 white	some structur and shine, some golden on them, moderate-better condition	many forams, moderate condition some broken ones	some small grey/brownish grains, some transpherent treads	100	108		0,03	3,55	
211-212		215/3/11-12	13 transpherent/white	27 white/grey/yellow	few forams, some structur and shine, some golden on them, moderate-better condition	many forams, moderate condition some broken ones	some small grey/brownish grains, some cylinder/grey cemented material	101	109		0,03	3,55	
221-222		215/3/21-22	27 white/transpherent	26 white/yellow/grey	many forams, some structur and shine, some golden on them, moderate-better condition	many forams, moderate condition some broken ones	some small grey/brownish grains, some cylinder/grey cemented material	102	110		0,03	3,55	
231-232		215/3/31-32	23 white/transpherent	23 white/yellow/grey	some structur and shine, some golden on them, moderate-better condition	many forams, moderate condition	some small grey/brownish grains, some cylinder/grey cemented material	103	111		-0,03	3,20	
241-242		215/3/41-42	23 white/transpherent	28 white/grey/yellow	some structur and shine, some golden on them, moderate-better condition	many forams, moderate condition	some small grey/brownish grains, some transpherent treads	104	112		0,10	3,52	
251-252		215/3/51-52	5 white	23 white/yellow/grey	very few forams, little structur and shine, moderate condition	few forams, moderate condition	some small grey/brownish grains, some cemeneted		113		-1,43	3,83	
261-262		215/3/61-62	20 white/transpherent	29 white/yellow/grey	few forams, some structur and shine, moderate condition	moderate condition	some small grey/brownish grains, some transpherent treads	105	114		-0,48	3,75	
271-272		215/3/71-72	10 white	22 white/yellow/grey	few forams, little structur and shine, moderate-bad condition	few forams, moderate condition	much small transpherent grains		115		-0,03	4,10	
281-282		215/3/81-82	31 white/transpherent	27 white/yellow/grey	many forams, some structur and shine, some golden on them, moderate condition	many forams, moderate condition	small grey/brownish grains	106	116		-2,51	4,08	
291-292		215/3/91-92	26 white/transpherent	22 white/yellow/grey	many forams, some structur and shine, some golden on them, moderate condition	few forams, moderate condition some broken	small grey/brownish grains	107	117		-0,17	3,31	
301-302	4	215/4/1-2	24 white/transpherent	26 white/yellow/grey	some structur and shine, moderate condition	few forams, moderate condition some broken	small grey/brownish grains	108	118		-0,74	4,29	
311-312		215/4/11-12	23 white/transpherent	24 white/yellow/grey	some structur and shine, moderate condition	few forams, moderate condition some broken	small grey/brownish grains	109	119		-0,07	4,42	
321-322		215/4/21-22	28 white/transpherent	10 white/yellow/grey	some structur and shine, some golden on some of then, moderate condition	few forams, moderate condition some broken	small grey/brownish grains, some cylinder/grey cemented material	110	120		-0,14	3,89	
331-332		215/4/31-32	25 white	24 white/yellow/grey	small sample, some structur and shine, golden on some of then, moderate condition	moderate condition	much small grey/brownish grains	111	121		-13,13	5,03	
341-342		215/4/41-42	33 white	7 white/yellow/grey	small sample, some structur and shine, moderate condition	few forams, moderate condition some broken	much small grey/brownish grains, some cylinder/grey cemented material	112					
351-352		215/4/51-52	30 white	28 white/grey/yellow	many forams small sample, some structur and shine, moderate condition	many forams small sample, moderate condition	much small grey/brownish grains	113	122		-4,25	4,85	
361-362		215/4/61-62	29 white	29 white/yellow/grey	many forams, some structur and shine, moderate condition	many forams, moderate condition	much small grey/brownish grains	114	123		-3,41	4,63	
371-372		215/4/71-72	35 white/transpherent	24 white/yellow/grey	many forams, some structur and shine, moderate-better condition	moderate condition	much small grey/brownish grains	115	124		-0,32	4,46	
381-382		215/4/81-82	24 white/transpherent	28 white/grey/yellow	some structur and shine, moderate-better condition	moderate condition	much small grey/brownish grains	116	125		-2,72	4,41	
391-392		215/4/91-92	34 transpherent/white	40 white/grey/yellow	many forams small sample, some structur and shine, moderate-better condition	many forams small sample, moderate condition	much small grey/brownish grains	117	126		-0,33	3,82	
401-402	5	215/5/1-2	21 white/transpherent	28 white/grey/yellow	some structur and shine, moderate-better condition	many forams, moderate condition	much small grey/brownish grains	118	127		-0,43	2,83	
411-412		215/5/11-12	21 white/transpherent	27 white/grey/yellow	some structur and shine, moderate condition	many forams, moderate condition	much small grey/brownish grains	119	128		-3,37	4,80	
421-422		215/5/21-22	23 white/transpherent	23 white/yellow/grey	some structur and shine, moderate-better condition	many forams, moderate condition	much small grey/brownish grains	120	129		-2,35	4,98	
431-432		215/5/31-32	23 white/transpherent	26 white/yellow/grey	some structur and shine, moderate condition	many forams, moderate condition	much small grey/brownish grains	121	130		-4,63	4,81	
441-442		215/5/41-42	27 white/transpherent	26 white/yellow/grey	some structur and shine, moderate condition	many forams, moderate condition	much small grey/brownish grains	122	131		-2,20	4,92	
451-452		215/5/51-52	24 white/transpherent	34 white/yellow/grey	some structur and shine, moderate-better condition	many forams, moderate condition	much small grey/brownish grains	123	132		-0,90	4,65	
461-462		215/5/61-62	4 transpherent/white	26 white/yellow/grey	very few forams, some structur and shine, better condition	moderate condition	much small grey/brownish grains, some bigger grey grains also		133		-1,42	4,67	
471-472		215/5/71-72	29 white/transpherent	29 white/yellow/grey	few forams bigg sample, some structur and shine, moderate-better condition	moderate condition	much small grey/brownish grains, some black grains, some bigger grains		134		-2,21	4,35	
481-482		215/5/81-82	27 white/transpherent	35 white/yellow/grey	some structur and shine, moderate-better condition	many forams, moderate condition	much small grey/brownish grains	124	135		-0,14	4,70	
491-492		215/5/91-92	5 white/transpherent	31 white/yellow/grey	some structur and shine, moderate condition	many forams, moderate condition	much small grey/brownish grains		136		-2,93	4,67	
501-502	6	215/6/01-02	0	29 white/yellow/grey		moderate condition	much small grey/brownish grains		137		-8,98	5,29	

Core HH-13-217 GC 22			Foraminifera (counting and color)		Forams describtion			Isotop analysis (marked samples)		Isotop analysis result (of marked samples)		
										Benthic	Planktic	
			Benthic	Planktic	Benthic	Planktic	Grains (>100µm)	Benthic	Planktic	C. neoteretis	N. pachyderma	
sample depth (cr	section	marked as (or	Cassidulina neotere	Neogloboquedrina pachyde	Cassidulina neoteretis	Neogloboquedrina pachyderma	Describtion	C. neoteretis	N. pachyderma		d13C VPDB [‰	d18O VPDB [‰]
1-2	1	217/1/1-2	12 transpherent	27 white/grey	very small sample, some structur and shine, better-mod	many forams very small sample, moderate condition	Small grey/brownish grains	125	138		0,36	3,39
11-12		217/1/11-12	28 white/transphere	29 white	little structur and shine, moderate condition	moderate condition	Small grey/brownish grains, lots of transpherent treads	126	139		0,43	3,26
21-22		217/1/21-22	25 white/transphere	32 white	little structur and shine, moderate condition	moderate condition some holes	Small grey/brownish grains, lots of transpherent treads	127	140		0,34	3,41
31-32		217/1/31-32	25 transpherent	39 white/grey	some structur and shine, moderate-better condition	many forams, moderate condition	Small grey/brownish grains, lots of transpherent treads	128	141		0,20	3,30
41-42		217/1/41-42	20 transpherent/whi	25 white	some structur and shine, moderate condition	many forams, moderate condition	Small grey/brownish grains, lots of transpherent treads	129	142		0,74	3,50
51-52		217/1/51-52	19 white/transphere	30 white	some structur and shine, moderate condition	many forams, moderate condition some holes	Small grey/brownish grains, lots of transpherent treads	130	143		0,77	3,55
61-62		217/1/61-62	22 white/transphere	30 white	little structur and shine, moderate condition	many forams, moderate condition some holes	Small grey/brownish grains, lots of transpherent treads	131	144		0,63	3,47
71-72		217/1/71-72	11 white/transpheren	33 white	little structur and shine, moderate condition	many forams, moderate-better condition	Small grey/brownish grains		145		0,63	3,64
81-82		217/1/81-82	24 transpherent	25 white	some structur and shine, moderate-better condition	many forams, moderate-better condition	Small grey/brownish grains, lots of transpherent treads	132	146		0,40	3,20
91-92		217/1/91-92	24 transpherent/whi	24 white/yellow	some structur and shine, moderate-better condition	many forams, moderate condition	Small grey/brownish grains, lots of transpherent treads	133	147		0,63	3,36
101-102	2	217/2/1-2	21 transpherent/whit	24 yellow/white	some structur and shine, moderate-better condition	moderate-better condition	Small grey/brownish grains, lots of transpherent treads	134	148		0,45	3,55
111-112		217/2/11-12	20 transpherent	22 white/grey	little structur and shine, moderate condition	many forams, moderate condition	Small grey/brownish grains, lots of transpherent treads	135	149		0,46	3,23
121-122		217/2/21-22	24 transpherent	24 white	little structur and shine, moderate condition	many forams, moderate-better condition	Lots of small grey/brownish grains	136	150		0,48	3,29
131-132		217/2/31-32	19 transpherent	30 white	little structur and shine, moderate condition	many forams, moderate condition	Lots of small grey/brownish grains	137	151		0,39	3,14
141-142		217/2/41-42	25 transpherent	27 white	little structur and shine, moderate condition	many forams, moderate condition	Lots of small grey/brownish grains	138	152		0,55	3,14
151-152		217/2/51-52	26 transpherent	27 white	little structur and shine, moderate condition	many forams, moderate condition	Lots of small grey/brownish grains	139	153		0,27	3,05
161-162		217/2/61-62	20 transpherent/whi	22 white	some structur and shine, moderate-better condition	moderate condition	Small grey/brownish grains, some cemented		154		0,31	2,83
171-172		217/2/71-72	20 transpherent/whi	33 white/grey	some structur and shine, moderate condition	moderate condition	Small grey/brownish grains, some cemented	140	155		0,12	3,03
181-182		217/2/81-82	26 transpherent/whit	31 white	little structur and shine, moderate condition	moderate condition	Small grey/brownish grains, some cemented	141	156		0,20	4,03
191-192		217/2/91-92	9 transpherent/whit	22 white	few forams, little structur and shine, moderate condition	many forams, moderate condition	Small grey/brownish grains, some cemented		157		0,01	2,96
201-202	3	217/3/1-2	18 transpherent/whit	22 white	little structur and shine, moderate condition	moderate condition	Small grey/brownish grains, some cemented		158		-0,04	3,02
211-212		217/3/11-12	22 transpherent/whi	28 white	little structur and shine, moderate condition	many forams, moderate condition	Small grey/brownish grains, some cemented	142	159		-0,23	2,93
221-222		217/3/21-22	20 transpherent/whi	24 white	little structur and shine, moderate condition	many forams, moderate condition	Small grey/brownish grains	143	160		-0,05	3,16
231-232		217/3/31-32	22 white/transphere	22 white	little structur and shine, moderate condition	many forams, moderate condition	Small grey/brownish grains	144	161		-0,05	3,25
241-242		217/3/41-42	21 transpherent/whit	22 white	little structur and shine, moderate condition	many forams, moderate condition	Small grey/brownish grains	145	162		0,03	3,49
251-252		217/3/51-52	6 transpherent/whit	28 white	little structur and shine, moderate condition	many forams, moderate condition	Small grey/brownish grains		163		0,12	3,74
261-262		217/3/61-62	20 transpherent/whi	22 white/yellow	little structur and shine, moderate condition	moderate condition	Small grey/brownish grains		164		0,10	3,58
271-272		217/3/71-72	22 transpherent/whi	27 white	little structur and shine, moderate condition	many forams, moderate condition	Small grey/brownish grains	146	165		0,04	3,87
281-282		217/3/81-82	16 transpherent/whit	25 white/grey	little structur and shine, moderate condition	many forams, moderate condition	Small grey/brownish grains	147	166		0,12	3,18
291-292		217/3/91-92	0	2 white	small sample	very few forams small sample, moderate condition	Small transpherent and white grains					
301-302	4	217/4/1-2	25 transpherent/whi	33 white/yellow	many forams small sample, some structure and shine, n	many forams small sample, moderate condition	Small grey/brownish grains	148	167		-0,16	4,43
311-312		217/4/11-12	23 transpherent/whi	23 white	small sample, some structure and shine, moderate-bett	small sample, moderate condition	Small grey/brownish grains, some transpherent and white gi	149	168		-0,12	4,27
321-322		217/4/21-22	22 transpherent/whi	25 white	some structure and shine, moderate-better condition	moderate-better condition	Small grey/brownish grains	150	169		0,03	4,14
331-332		217/4/31-32	23 transpherent/whi	28 white	many forams, some structure and shine, moderate-bett	many forams, moderate condition	Small grey/brownish grains, some transpherent grains	151	170		-0,07	4,24
341-342		217/4/41-42	23 transpherent/whi	24 white/grey	little structure and shine, moderate condition	moderate condition	Small grey/brownish grains, some transpherent grains	152	171		-0,03	4,24
351-352		217/4/51-52	9 transpherent/whit	24 white	some structure and shine, moderate condition	moderate condition	Small grey/brownish grains, some transpherent grains		172		-0,09	4,49
361-362		217/4/61-62	22 transpherent/whi	14 white	small sample, some structure and shine, moderate-bett	small sample, moderate condition some holes	Small grey/brownish grains, some transpherent grains	153	173		-0,23	4,36
371-372		217/4/71-72	35 transpherent/whi	23 yellow	small sample many forams, some structure and shine, n	small sample, moderate condition some holes	Small grey/brownish grains	154	174		-0,27	4,28
381-382		217/4/81-82	2 transpherent/whit	22 white	small sample very few forams, some structure and shine	small sample, moderate condition some holes	Small grey/brownish grains		175		-0,35	4,33
391-392		217/4/91-92	0	30 white		moderate condition	Small grey/brownish grains		176		-0,08	4,66
401-402	5	217/5/1-2	2 white	52 white	very few forams, little structure and shine, moderate co	moderate-better condition	Small grey/brownish grains		177		-0,06	4,53
411-412		217/5/11-12	25 white/transphere	28 white	little structure and shine, moderate condition	moderate-better condition	Small grey/brownish grains	155	178		-0,10	4,53
421-422		217/5/21-22	23 white	23 white	big sample, some structure and shine, moderate condit	moderate-better condition	Small grey/brownish grains, some transpherent and white gi	156	179		-0,10	4,81
431-432		217/5/31-32	10 white	25 white	big sample, little structure and shine, moderate-bad con	moderate condition	Small grey/brownish grains, some transpherent and white gi	157	180		-0,10	4,72
441-442		217/5/41-42	21 white/transpheri	25 white	some structure and shine, better condition	moderate condition	Small grey/brownish grains	158	181		-0,17	4,46
451-452		217/5/51-52	1 transpherent	5 white	some structure and shine, moderate condition	moderate condition	Small transpherent and white grains					
461-462		217/5/61-62	3 white/transpheren	25 white	little structure and shine, moderate condition	moderate condition	Small grey/brownish grains, some transpherent and white grains		182		0,02	4,17
471-472		217/5/71-72	0	25 white/yellow		moderate condition	Small grey/brownish grains, some transpherent and white grains		183		0,01	4,26
481-482		217/5/81-82	0	1 white		moderate condition	Small transpherent grains					
491-492		217/5/91-92	17 transpherent/whit	50 white	little structure and shine, moderate condition	moderate condition	Small grey/brownish grains, some transpherent grains	159	184		0,11	4,60
501-502	6	217/6/1-2	0	15 yellow/grey		moderate condition	Lots of small transpherent grains		187		-0,16	4,83
511-512		217/6/11-12	0	21 yellow/grey		moderate condition	Lots of small transpherent grains		188		-0,11	4,63
521-522		217/6/21-22	0	23 grey/yellow		moderate condition some holes	Lots of small transpherent grains		189		0,00	4,54
531-532		217/6/31-32	0	25 grey/yellow		moderate-bad condition some holes	Lots of small transpherent grains		190		-0,02	4,68
541-542		217/6/41-42	0	24 white/yellow		moderate condition	Lots of small transpherent grains		191		0,34	4,55
551-552		217/6/51-52	1 white	20 white/yellow	very few forams, little structure and shine, bad condition	moderate condition	Lots of small transpherent grains		192		0,19	4,53
561-562		217/6/61-62	0	16 white/yellow		moderate condition	Lots of small transpherent grains		193		-0,11	4,15
571-572		217/6/71-72	0	21 grey/white		moderate-bad condition	Lots of small transpherent grains		194		0,14	4,38
581-582		217/6/81-82	2 white	25 white/yellow/grey	very few forams, little structure and shine, bad condition	moderate condition	Lots of small transpherent grains		195		0,17	4,47

References:

Aloisi, G., Pierre, C., Rouchy, J.-M., Foucher, J.-P., Woodside, J., & Party, t. M. S. (2000). Methane-related authigenic carbonates of eastern Mediterranean Sea mud volcanoes and their possible relation to gas hydrate destabilisation. *Earth and Planetary Science Letters, 184*, 321-338.

Armstrong, H. A., & Braiser, M. D. (2013). *Microfossils* (second edition ed.): 25-35, 142-188, Elsevier.

Boetius, A., Ravenschlag, K., Schubert, C. J., Rickert, D., Widdel, F., Gieseke, A., . . . Pfannkuche, O. (2000). A marine microbial consortium apparently mediating anaerobic oxidation of methane. *Nature, 407*(6804), 623-626.

Bradley, R. S. (2015). *Paleoclimatology reconstructing climates of the quaternary* (third ed.). Massachusetts: 141-145, 197-210 Elsevier.

Brix, H., & Gerdes, R. (2003). North Atlantic Deep Water and Antarctic Bottom Water: Their interaction and influence on the variability of the global ocean circulation. *Journal of geophysical research, 108*.

Carstens, J., Hebbeln, D., & Wefer, G. (1997). Distribution of planktic foraminifera at the ice margin in the Aictic (Fram Strait) *Marine Micropaleontology, 29*, 257-269.

Consolaro, C., Rasmussen, T. L., & Panieri, G. (2018). Palaeoceanographic and environmental changes in the eastern Fram Strait during the last 14,000 years based on benthic and planktonic foraminifera. *Marine Micropaleontology, 139*, 84-101.

Ehrenberg. (1996). Neogloboquadrina pachyderma.

Hovland, M., & Judd, A. G. (1988). seabed pockmarks and seepages impact on geology, biology and marine environments. *Graham and Trotman*, 1-5, 140-142.

Howe, J., Piotrowski AM, Noble TL, Mulitza S, Chiessi CM, & North, B. G. (2016). North Atlantic Deep Water Production during the Last Glacial Maximum. *Nature communications, 7*(11765).

Howe, J. A., Shimmield, T. M., Harland, R., & Eyles, N. (2008). Late Quaternary contourites and glaciomarine sedimentation in the Fram Strait. *Sedimentology, 55*(1), 179-200.

Jacob, D. E., Wirth, R., Agbaje, O. B. A., Branson, O., & Eggins, S. M. (2017). Planktic foraminifera form their shells via metastable carbonate phases. *Nature communications, 8*(1265).

Jessen, S. P., Rasmussen, T. L., Nielsen, T., & Solheim, A. (2010). A new late Weichselian and Holocene marine chronology for the western Svalbard slope 30, 000-0 cal years BP. *Quaternary Science Reviews 29*, 1301-1312, Elsevier.

Johnson. (2015). The potential for abiotic methane in arctic gas hydrates. *Fire in the ice newsletter, 16*(1), 9-12.

Johnson, J. E., Phillips, S., Panieri, G., Knies, J., Sauer, S., Schneider, A., Mienert, J. (2014). Tracking paleo-SMT positions using a magnetic susceptibility proxy approach from sediments on the Arctic Vestnesa Ridge, offshore western Svalbard, *EGU General assembly*.

Judd, A. G., Hovland, M., Dimitrov, L. I., Garci ´A Gil, S., & Jukes, V. (2002). The geological methane budget at Continental Margins and its influence on climate change. *Geofluids, 2*, 109-126.

Katz, M. E., Benjamin, C. S., Franzese, A., Hönisch, B., Miller, K. G., Rosenthal, Y., & Wright, J. D. (2010). Traditional and emerging geochemical proxies in foraminifera. *Journal of Foraminiferal Research, 40*(2), 165-192.

Klitzke, P., Luzi-Helbing, M., Schicks, M., Cacacea, A. B., ., Jacquey, J., Sippel., M., Faleide. (2016). Gas Hydrate Stability Zone of the Barents Sea and Kara Sea Region. *Energy Procedia, 97*, 302-309, Elsevier.

Knies, J., & Stein, R. (1998) New aspects of organic carbon deposition and its paeoceanographic implications along the northern Barents Sea margin during the last 30,000 years. *Paleoceanography, 13(4)*, 384-394.

Malinverno, A. (2010). Marine gas hydrates in thin sand layers that soak up microbial methane. *Earth and Planetary Science Letters, 292*(3), 399-408.

Miniert, J., Almestad, J., Plaza-Faverola, A., Johnson, J., Franek, P., , Urban, P., Osti, G., Olsen, B. (2013). *Cruise report FF Helmer Hansen*.

Nieuwenhove, N. V., Bauch, H. A., & Matthiessen, J. (2008). Last interglacial surface water conditions in the eastern Nordic Seas inferred from dinocyst and foraminiferal assemblages. *Marine Micropaleontology, 66*(3), 247 - 263.

Panieri, G., Graves, C. A., & James, R. H. (2016). Paleo-methane emissions recorded in foraminifera near the landward limit of the gas hydrate stability zone offshore western Svalbard. *Geochemistry, Geophysics, Geosystems, 17*, 203-212.

Panieri, G., Lepland, A., Whitehouse, M. J., Wirth, R., Raanes, M. P., James, R. H., . . . Crémière. (2016). Diagenetic Mg-calciteovergrowths on foraminifera testsin the vicinity of methane seeps. *Elsevier/ Earth planetary science letters, 458*, 203-212.

Pearson, P. N. (2012). Oxygen isotope in foraminifera: overview and historical review. *The Paleontological Society, 18*, 1-38.

Plaza-Faverola, A., Bünz, S., Johnson, J. E., Chand, S., Knies, J., Mienert, J., & Franek, P. (2015). Role of tectonic stress in seepage evolution along the gas hydrate-charged Vestnesa Ridge, Fram Strait. *Geophysical Research Letters, 42*, 1-10.

Rasmussen, T., & Thomsen, E. (2008). Warm Atlantic surface water inflow to the Nordic seas 34-10 calibrated ka B.P. *Paleoceanography, 23*(1), 1201.

Ravelo, A. C., & Hillaire-Marcel, C. (2007). Chapter Eighteen The Use of Oxygen and Carbon Isotopes of Foraminifera in Paleoceanography. *Developments in Marine Geology*, in *Proxies in Late Cenozoic Paleoceanography, 1*, 735-764, edited by C. Hillaire-Marcel and A. de Vernal, Elsevier Science & Technology, Amsterdam, The Netherlands.

Rudels, B. (2015). Arctic Ocean circulation, processes and water masses: A description of observations and ideas with focus on the period prior to the International Polar Year 2007–2009. *Progress in Oceanography, 132*, 22-67.

Ruppel, C. D., & Kessler, J. D. (2017). The interaction of climate change and methane hydrates. *Reviews of Geophysics, 55*, 126-168.

Schiebel, R., & Hemleben, C. (2005). Modern Planktic Foraminifera. *Paläontologische Zeitschrift, 79*, 135-148.

Schiermeier, Q. (2008). Fears surface over methane leaks. *Nature News, 455*(7213), 572-573.

Schneider, A., Panieri, G., Lepland, A., Consolaro, C., Crémière, A., Forwick, M., Knies, J. (2018). Methane seepage at Vestnesa Ridge (NW Svalbard) since Last Glacial Maximum. *Quaternary Science Reviews, 193*, 98-117, Elsevier.

Schneidera, A., Crémièrea, A., Panieria, G., Leplanda, A., & Kniesa, J. (2017). Diagenetic alteration of benthic foraminifera from a methane seep site on Vestnesa Ridge (NW Svalbard). *Deep-sea research 1, 123*, 22-34, Elsevier.

Smith, A. J., Mienert, J., Bünz, S., & Greinert, J. (2014). Thermogenic methane injection via bubble transport into the upper Arctic Ocean from the hydrate‐charged Vestnesa Ridge, Svalbard. *Geochem. Geophys. Geosyst, 15*(5), 1945-1959.

Sundh, I., Mikkelä, C., Nilsson, M., & Svensson, B. H. (1995). Potential aerobic methane oxidation in a Sphagnum-dominated peatland—Controlling factors and relation to methane emission. *Soil Biology and Biochemistry*, *27*(6), 829-837.

Vogt, P., Gardner, J., & Crane, K. (1999). The Norwegian–Barents–Svalbard (NBS) continental margin: Introducing a natural laboratory of mass wasting, hydrates, and ascent of sediment, pore water, and methane. *Geo-Marine Letters*, *19*(2), 2-21.

Vogt, P. R., Crane, K., Sundvor, E., Max, M. D., & Pfirman, S. L. (1994). Methane-generated(?) pockmarks on young, thickly sedimented oceanic crust in the Arctic: Vestnesa ridge, Fram strait. *Geology*, *22*(3), 255-258.

Vorren, T. O., Bergsager, E., Dahl-Stamnes, Ø. A., Holter, E., Johansen, B., Lie, E., & Lund, T. B. (1990). *Arctic Geology and Petroleum Potential.* Paper presented at the Norwegian Petroleum Society Conference, Tromsø.

Whiticar, M. J. (1999). Carbon and hydrogen isotope systematics of bacterial formation and oxidation of methane. *Chemical Geology, 161*, 291-314.

Zamelczyk, K., Rasmussen, T. L., Husum, K., & Hald, M. (2013). Marine calcium carbonate preservation vs. climate change over the last two millennia in the Fram Strait: Implications for planktic foraminiferal paleostudies. *Marine Micropaleontology, 98*, 14-27.

Zehnder, A. J. B., & Brock, T. D. (1979). Methane Formation and MethaneOxidation by Methanogenic Bacteria. *Journal of bacteriology*, *137*(1), 420-432.